Can the Urban Poor Avoid Flood Risks? The Case of Cape Town, South Africa*

Paolo Avner, Charlotte Liotta, Thomas Monnier, Basile Pfeiffer, Claus Rabe, Harris Selod, Vincent Viguié†

May 15, 2025

Click here for the latest version

Abstract

In low- and middle-income country cities, poor households often reside in unattractive locations, including flood-prone areas. This can be due to poor information about flood risks or acceptance of these risks in the face of lower housing prices. Poor households are also more vulnerable to floods than richer households given the low-quality housing they occupy. Does information on flood risks help households make better location and housing choices? To what extent will these choices be revised with increased flood risks from climate change? To answer these questions, we develop a polycentric urban economics model with heterogenous income groups, formal and informal housing, and flood risks. The model is calibrated to Cape Town (South Africa) and simulations are run to assess the impact of flood risks on land values and income segregation within the city, distinguishing between the effects of three types of floods (fluvial, pluvial, and coastal). Although total damages from floods are greater for rich households, they represent a larger relative share of poor households' incomes. Better information encourage the adaptation of poor households up to a certain point, and this allows them to mitigate most of the adverse consequences from climate change. Considering the different nature of flood types is key to understand their responses.

Keywords: floods, adaptation, informal housing
JEL Classification: Q51, Q54, R14, R31

*We thank the City of Cape Town for its support and facilitation of access to the data used in this paper. We are especially grateful to Amrish Bisoon, Hugh Cole, Paul Court, Robert McGaffin, Elmarie Nel, Jodie Posen, Kristoff Potgieter, Carol Wright, and all participants to the World Bank technical assistance organized as part of the Resilience Pillar of the Cities Support Program led by the National Treasury of the Government of South Africa. We are also indebted to Haroon Bhorat, Lukasz Grzybowski, Andrew Kerr, Martine Visser, and other people at the University of Cape Town for their valuable feedback. Funding from the Swiss State Secretariat for Economic Affairs is gratefully acknowledged.

†Avner: World Bank, GFDRR, pavner@worldbank.org; Liotta: Universitat Autònoma de Barcelona, ICTA, charlotte.liotta@uab.cat; Monnier: CREST, Ecole Polytechnique, IP Paris, thomas.monnier@ensae.fr; Pfeiffer: Inspection Générale des Finances; Rabe: Palmer Development Group, claus@pdg.co.za; Selod: World Bank, DEC, thomas.monnier@ensae.fr; Viguié: Ecole des Ponts ParisTech, CIRED, viguie.cired@gmail.com.

1 Introduction

In low- and middle-income countries, urban growth can be accompanied by greater vulnerability of poor households who tend to settle in flood-prone areas. In this paper, we propose the first urban simulation model that simultaneously accounts for all three types of flood risks (fluvial, pluvial, and coastal). Accounting for the whole range of flood risks makes it possible to assess how they differentially impact cities, so as to design better targeted policy responses.

As our model ambitions to offer a realistic representation of a low- and middle-income country city, it is important to account for key features such as income heterogeneity and the coexistence of formal and informal housing (including settlements erected in the backyard of public housing units). Building on a simplified version of previous work that was made on the city of Cape Town (Pfeiffer *et al.*, 2025), we directly apply a discrete two-dimensional version of the standard urban monocentric model (Fujita, 1989) on a grid of pixels, and simulate developers' construction decisions along with households' housing and location choices at a distance from multiple employment subcenters. At the same time, we account for land-use and building regulations, natural constraints, and exogenous amenities. This approach has been shown to have a strong predictive power in terms of urban patterns across the world (Liotta *et al.*, 2022).

We add flood risks to this modeling infrastructure by considering the probability of flood occurrence in each grid cell, and the corresponding damages caused to housing structures and contents. We consider that these are the most direct channels through which flood risks affect city patterns over the long term (Merz *et al.*, 2010; Pharoah, 2014; Mosimann *et al.*, 2018). Agents internalize these risks (or not) by considering the expected annual damage value (based on probabilistic flood maps) as an added term in the depreciation of their housing capital and quantity of goods consumed (Huizinga *et al.*, 2017). This extends the framework in Avner *et al.* (2022) by incorporating the impact of flood damages in both housing supply and demand.

We further distinguish between fluvial, pluvial, and coastal floods. Typically, fluvial floods are water overflows from rivers, whereas pluvial floods designate surface water floods or flash floods, caused by extreme rainfall independently of an overflowing water body. Coastal floods encompass storm surges, periodic tides, and gradual sea-level rise. In our model, flood risks do not only affect population and structures through their direct exposure to floods, but the city as a whole through equilibrium effects (i.e., with endogenous housing prices and sorting of the population across the city): the double vulnerability of poor households living in low-quality housing in flood-prone areas is especially important in this regard.

As a proof of concept, we present two comparative statics: one comparing scenarios with and without flood risk anticipation, then another one comparing scenarios with and without climate change. Although total damages from floods are greater for rich households (with a higher propensity to live on the coast), they represent a larger relative share of poor households' incomes (who therefore tend to react more strongly to flood risks). Better information encourages their relocation outside flood-prone zones and lowers their willingness to pay for exposed housing. However, affordable and protected areas may also be located far from job centers: this underlines the fundamental trade-off poor households face between social vulnerability and economic opportunities, and explains why they cannot entirely move away from flood risks. Most of the effect comes from households avoiding localized fluvial flood zones with acute destruction risks. On the contrary, pluvial flood zones are typically more widespread, with lower destruction risks. This explains why, in the face of climate change, households are able/willing to mitigate most of the adverse consequences in fluvial, but not in pluvial flood zones.

We insert ourselves in a long thread of land use and transport integrated models (LUTI) applied to the evaluation of urban climate policies in various economic contexts. For instance, Viguié & Hallegatte (2012) look at trade-offs and synergies between a greenbelt policy, a flood zoning policy, and a transportation subsidy within the context of Paris (France). In the context of Buenos Aires (Argentina), Avner *et al.* (2017) also look at complementarities between a public transport subsidy, an income compensation scheme, and a construction subsidy scheme. At the global scale, Liotta *et al.* (2023b) compare the impacts of four representative urban climate policies: a bus rapid transit program, a fuel tax, a fuel efficiency improvement, and an urban growth boundary (UGB). More related to our work, Liotta *et al.* (2024) study the impact of a fuel tax on spatial inequalities in the context of Cape Town (South Africa). They find that the poorest households, living in informal settlements or subsidized housing, have few or no ways to adapt to changes in fuel prices by changing housing type, adjusting their location or housing consumption, or shifting transportation modes. Complementary policies promoting a functioning labor market that allows people to change jobs easily, affordable public transportation, or subsidies helping poor households to rent houses closer to employment centers are also shown to improve the social acceptability of climate policies. In the current paper, we rather focus on the adaptation side of climate policies, and study the impact of flood risk information policies with climate change on spatial inequalities.

Our approach also relates to the so-called "quantitative urban models" (Redding & Rossi-Hansberg, 2017), which have been increasingly applied to emerging country contexts (Sturm *et al.*, 2023). Apart from the fact that we allow for an endogenous city fringe (which matters in the presence of a strong population growth), the main difference with these studies is that we consider job locations and (estimated) wages as exogenous. We do not see this simplification as a strong limitation given that floods generally do not lead to massive displacements of economic activity (Kocornik-Mina *et al.*, 2020). Besides, it allows for a more tractable model, with typically more dimensions of heterogeneity and a more granular geography. To the best of our knowledge, we are also the first to propose a realistic urban simulation model that integrates all types of flood risks within an internal city structure. Some quantitative urban models address coastal risks (Lin *et al.*, 2024; Balboni, 2025). These models focus on the productive aspects of the economy and primarily consider sea-level rise (linked to climate change), without accounting for other components of coastal risks such as tides and storm surges. The literature on these effects (focusing on the formal housing market) is mostly in reduced form (Ortega & Taşpınar, 2018; Muller & Hopkins, 2019; Ellen & Meltzer, 2024). A notable exception is Varela (2023), which uses a residential segregation model to explain the heterogeneous price recoveries following a hurricane. The economic literature on fluvial and pluvial risks appears to be less extensive, likely due to the periodic (and thus predictable) nature of these phenomena, which complicates causal analysis.

Section 2 presents stylized facts regarding flood risks in Cape Town. Section 3 presents the data. Section 4 presents the model and Section 5 how it is estimated. Section 6 presents the model results for two sets of comparative statics: the first one introduces information on flood risks, and the second one the effects of climate change. Section 7 concludes.

2 Context

Cape Town, a sprawling city of four million inhabitants is located on a broad, sandy plain connecting the mountainous Cape peninsula to the mainland. It is among the cities most affected by fluvial and pluvial flood risks in Sub-Saharan Africa, with 160,000 households directly exposed and average annual damages estimated at almost \$16 million (World Bank, 2022). Damages from coastal floods (storm surges and periodic tides) are less important in absolute terms (around \$370,000 annually), but could sharply increase and affect more people with climate change and sea-level rise (Hallegatte *et al.*, 2013). For reference, we show a map of Cape Town's major flood plains in Figure 1 below.

Figure 1: Cape Town's major flood plains

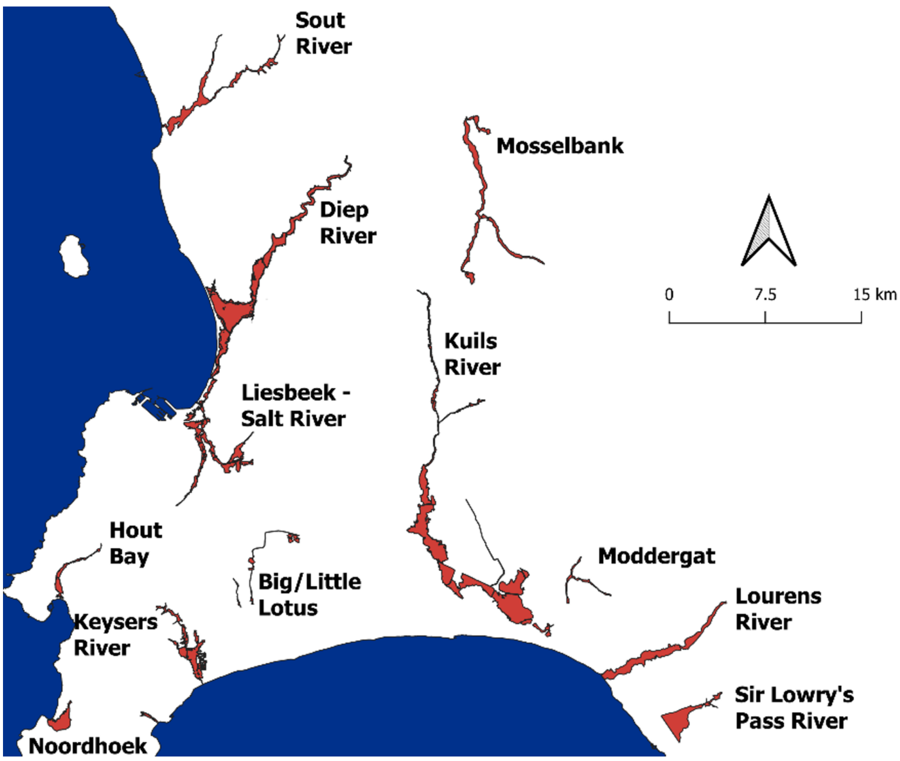

A large fraction of the population resides in the Cape Flats, a predominantly low-lying area of about 25x25km where approximately 200,000 poor households (15-20% of the population) live in informal settlements. The hydrology of the Cape Flats renders poor households living in informal settlements vulnerable to both fluvial and pluvial flooding. Fluvial flooding is episodic, typically more intense, and localized along Cape Town's four perennial rivers and stormwater channels. Pluvial flooding, on the other hand, is persistent and widespread across the Cape Flats area: the vast network of seasonal rivers, streams, and wetlands transecting the area is inundated for a few weeks annually during the rainy winter season. From there, drainage is encumbered by flat terrain and a water table lying between 1-3m from the surface in the dry summer months, but rises by between 1-2m during winter, causing "rising water" or "seepage" in topographic depressions. The impact of hydrology on households is aggravated by inadequate drainage infrastructure, which leads to localized ponding. Figure 2 below shows a more detailed map of the Cape Flats and their exposure to floods in flood-prone depressions (green areas) and flood-prone riverines (blue areas). It also shows the location of informal settlements (dark grey and black areas) in proximity of these zones.

Figure 2: Flood-prone zones in the Cape Flats

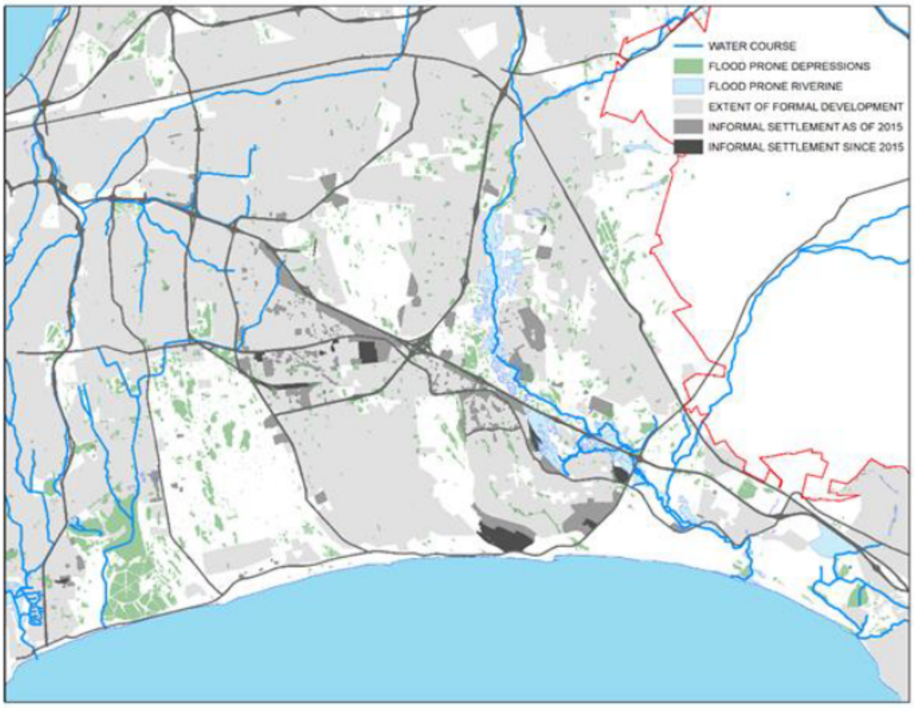

The magnitude of the flood impacts on poor households is determined both by nature and by human behavior. The main human cause of impact is the massive, informal occupation of large areas of flood-prone wetlands and detention ponds by poor households who build vulnerable structures from corrugated iron sheets. The propensity for households to locate in flood-prone areas is not incidental, but attributable to the fact that formal development is prohibited in flood-prone areas, leaving vacant remnants of land throughout the Cape Flats area. Furthermore, South African courts have pronounced that local authorities are not allowed to evict illegal land occupants from erected structures unless alternative accommodation is provided. Land occupation events typically occur in the run-up to winter since local authorities are reluctant to evict residents during winter on humanitarian grounds. In the remainder of this paper, we will consider tolerance for informal settlement zones as an exogenous factor.

With population growth and these ongoing spatial dynamics, the extent of informal settlements in flood-prone areas has increased from 17ha in 1995 to 147ha in 2020, and the corresponding number of vulnerable households from roughly 2,500 to 15,000 (based on aerial imagery). In what follows, we uncover the economic mechanisms behind such development, and assess how flood damages are likely to evolve following adaptation to better information and climate change.

3 Data

This section starts by presenting the data we use to estimate our model, and how we process it.

Grid We use a grid of 500x500m resolution, that encompasses the whole urban area and corresponds to the grid that the City of Cape Town uses for planning purposes. All other datasets are either spatially aggregated or disaggregated to fit the grid.

Figure 3: Expected capital depreciation rate due to floods (housing contents)

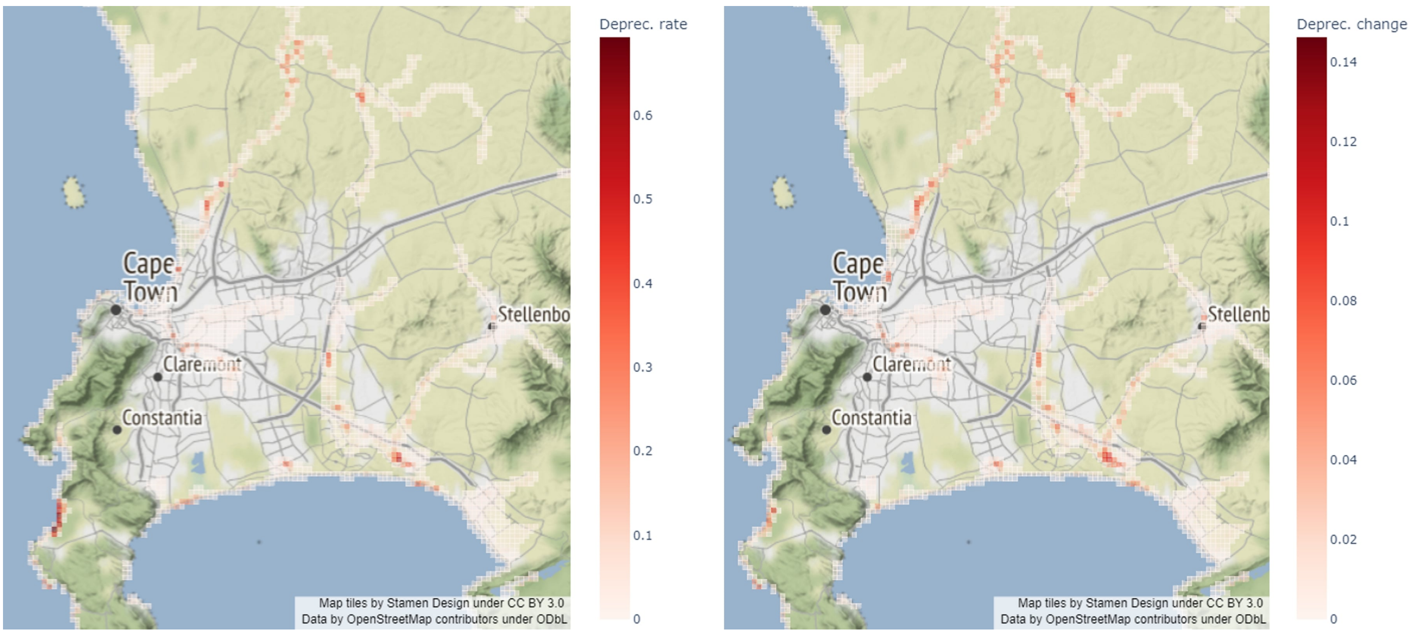

Note: The map on the left shows the values at baseline. The map on the right shows the change (in absolute terms) when considering climate change.

Flood data We use the FATHOM (Sampson *et al.*, 2015) and the Deltares (2021) data, two global spatial datasets of flood hazards. They provide flood water extent and depth for respectively pluvial/fluvial and coastal hazard scenarios, expressed as "return periods", which indicate the likely frequency of occurrence (i.e., once every number of years) for each flood event category. When overlapping, we consider the maximum flood depth across flood types as water would typically flow to other areas instead of piling up. The data are at a 3 arc-second (approximately 90m) resolution.

For reference, the climate conditions used to produce the flood maps are the ones prevailing in 2018, which we assume to be roughly in line with the ones prevailing at our baseline year (2011). Because our geographic units are 30 times larger than the units used in the raw flood maps, the flood data that we use is sufficiently granular to capture flood impacts at the grid cell level. Note however that we use the "undefended" versions of the datasets, i.e. the ones that do not account for infrastructure and other potential protection investments affecting flood hazards. This is because the global data is not precise enough to properly account for their spatial distribution at the local level. An exception we make is for the presence of drainage systems, which we assume to be linked with formal concrete housing structures: such dwelling units will not be affected by the least severe (but more frequent) flood events. We intend to prioritize the simulation of other protective investments in future work, as they are of the utmost policy relevance.

In every grid cell, the flood data is converted into an expected fraction of capital destroyed, collapsing all return periods into one annualized value. To do so, we borrow "structural" damage functions by housing type from Englhardt *et al.* (2019) that convert flood depth into building destruction shares. We also consider damages in terms of "contents", expressed as the fraction of (semi-)durable goods that households consume and that are vulnerable to floods. To obtain the expected fraction of contents destroyed, we use the flood depth-damage function proposed by De Villiers *et al.* (2007).

Finally, we consider how climate change might affect flood hazards. For coastal flood risks, we rely on specific flood maps provided by Deltares, that are based upon the IPCC's RCP 8.5 scenario projected onto the year 2050. Since the FATHOM data does not come with similar maps for pluvial/fluvial flood risks, we simply multiply all annual probabilities by 2 (i.e., we divide return periods by 2) as a proof of concept: this increase is of the same order of magnitude as the one observed for coastal flood risks. It should be noted that those scenarios are generally thought of as being relatively pessimistic.

To illustrate our approach, we represent in Figure 3 the spatial distribution of the flood-content depreciation rate (which does not vary across housing types), and how it changes with climate change (in absolute terms). As expected, flood exposure follows the coastline (for coastal flood risks), waterways (for fluvial flood risks), and topological depression areas (for pluvial flood risks). Note that this is only an intermediate output, as final damages will also depend on households' housing and location choices, depending on economic opportunities and real estate prices. The increase in risk also appears to be non-negligible, reaching more than 10 percentage points in most exposed zones.

Socioeconomic data The rest of the data is the same as in Pfeiffer *et al.* (2025). We refer the reader to this paper for more visualization of model inputs. The spatial distribution of the population is taken from the 2011 National Census and is used to close the model. We consider four housing types, namely formal private housing (FP), formal subsidized housing (FS), informal settlements (IS), and informal backyards (IB). We also define four income groups of interest by choosing income-group thresholds such that only the lowest income group is eligible for subsidized housing programs, and so that the two highest income groups are not observed to reside informally (but are distinguished to account for high income inequality).

We use the City of Cape Town's transport model to retrieve transport times and distances between pairs of transport zones for each transport mode and job locations, along with the estimated number of households per employment center and income group. The monetary transport costs are retrieved from additional external sources. We also use aggregate statistics on residence-workplace distances in Cape Town, derived from Cape Town's 2013 Transport Survey, to complete the estimation of households' expected income net of commuting costs (see Section 5).

Land availability is defined for each housing type. Areas of subsidized housing are identified from the cadastre of the City of Cape Town. The area available for backyard housing is estimated as the yard size of these units: in the context of Cape Town, most of so-called informal "backyarding" occurs in such precincts. Informal settlement areas are obtained from the characterization of enumeration areas (census blocks) in the 2011 Census: in the context of Cape Town, they correspond to peripheral, publicly-owned land originally reserved for future roads, social facilities, or public housing. It therefore makes sense to consider them as being exogenously given. Land available for formal private development corresponds to all land that is not constrained for housing construction (including exogenous commercial floor space). Additional height restrictions apply across the city.

The amenities that we consider include natural amenities (such as slope and proximity to the ocean) as well as urban amenities (such as the proximity to the historical center): we extract them from the City of Cape Town's open data portal, and take them as being exogenous (i.e., we do not endogenize them as a model residual) to precisely identify potential policy levers in future work. Pfeiffer *et al.* (2025) find that this does not lead to strong underfitting. Finally, we use property prices extracted from the City of Cape Town's geocoded dataset on property transactions for 2011, as well as data on dwelling sizes made available to us by the City of Cape Town. These will serve to estimate the parameters of the housing production technology used by formal private developers.

4 Model

4.1 Environment

We base ourselves on a simplified static version of the model from Pfeiffer *et al.* (2025) that we augment with flood risks. As in their framework, we consider that each grid cell in the city is indexed by a vector of coordinates $x = (x_1, x_2)$ and has an exogenous quantity of available land for residential development per housing type $h = FP, FS, IS, IB$, $L_h(x)$. In addition, each location is characterized by an exogenous amenity index $A(x)$ (centered around one), and an exogenous disamenity index $B_h(x)$ (below one) associated with informal housing types $h = IS, IB$. A minor change from Pfeiffer *et al.* (2025) is that the informal disamenity index now varies across space to better fit the overall population distribution. Then, the model focuses on heterogeneous households' housing and location choices, conditional on expected employment outcomes.

It is important to note that we concentrate on material damages of floods in the housing market. We do not address other potentially relevant risks, such as those affecting infrastructure (Hallegatte *et al.*, 2019), health (Picarelli *et al.*, 2017; Paterson *et al.*, 2018), or public services (Hammond *et al.*, 2015; Allaire, 2018). These extensions are left for future work.

Housing demand Households choose their consumption of composite good z and housing quantity q, along with their residential location x and housing type h, by maximizing Stone-Geary preferences:

$$U(z, q, x, h) = z^{\alpha}(q - q_0)^{1-\alpha} A(x) B_h(x) \tag{1}$$

where $0 < \alpha < 1$ is the composite good elasticity (or budget share), $1 - \alpha$ is the surplus housing elasticity, and $q_0 > 0$ is the basic need in housing.

In doing so, they face the following budget constraint, that also depends on their income group $i = 1, .., 4$ (from poorest to richest):

$$\begin{aligned} &\tilde{y}_i(x) + \mathbb{1}_{\{h=FS\}} \mu(x) Y R_{IB}(x) \\ &\quad = \left(1 + \gamma \rho^{content}(x)\right) z + q_h R_h(x) + \mathbb{1}_{\{h \neq FP\}} \left(\rho + \rho_h^{struct}(x) + \mathbb{1}_{\{h \neq FS\}} \delta\right) v_h \end{aligned} \tag{2}$$

In equation (2), the left-hand side stands for revenues, and the right-hand side for expenses. On the left-hand side, $\tilde{y}_i(x)$ is the expected income net of commuting costs for a household of income group i living in location x: since households choose their residential location ex ante, they consider the likelihood that they find employment (or not) in the surrounding job centers, along with the associated commuting costs and the (exogenous) income they would obtain given their income group at each specific workplace. This can also be rationalized ex post by considering that the equilibrium is a static representation of a life-cycle process in which households lose and change jobs (albeit not residential locations) over time.

When living in formal subsidized housing ($\mathbb{1}_{\{h=FS\}}$), households have the additional possibility to rent out an endogenous fraction $\mu(x)$ of their backyard of fixed size Y at the endogenous market rent $R_{IB}(x)$.

On the right-hand side, households need to pay for composite good z (whose price is normalized to one). γ is the fraction of (semi-)durable goods that is exposed to floods and that depreciates at rate $\rho^{content}(x)$: this corresponds to the expected fraction of capital destroyed from Figure 3. They also need to pay for housing quantity q_h at the endogenous annual rent $R_h(x)$. Although the housing consumption is a choice variable for $h = FP$, it is fixed for $h = FS, IS, IB$. We further assume that the rent is zero for $h = FS$. In practice, this means that it is always profitable for the poorest households to accept public housing offers. Therefore, in equilibrium, all formal subsidized housing will be provided until the rest of income group 1 is rationed out of this housing submarket.

We assimilate formal private residents to tenants who rent their housing from owner-developers who themselves buy the land from absentee landlords. This is without loss of generality when assuming no arbitrage between owning and renting, since the total price of housing (or land) can be recovered as the infinite sum of discounted future rents (and conversely). However, this affects whether the costs of construction and maintenance enter the demand- or supply-side of the model formulation, since we assume they are covered by owner-developers. Again, this is without loss of generality in competitive markets, since the standard tax incidence equivalence result holds. Because we assimilate informal dwellers to owner-developers (which is aligned with anecdotal evidence from the field), and subsidized housing dwellers to owner-occupiers (buying for free from public developers), only they will directly pay for the costs of maintenance (and construction in the case of informal dwellers). Also note that, in the case of informal settlements, absentee landlords can be assimilated to illegitimate squatter-coordinators on public land, who extract a rent-like payment from informal dwellers (Marx *et al.*, 2019).

Mathematically, they ($\mathbb{1}_{\{h \neq FP\}}$) all pay a fraction $\rho + \rho_h^{struct}(x)$ of building accounting value v_h (remember that this is fixed for $h \neq FP$), and informal dwellers ($h \neq FS$)) additionally pay for a fraction δ of this amount. ρ is the standard capital depreciation rate, and $\rho_h^{struct}(x)$ is the added expected fraction of capital destroyed due to floods. δ is the cost of capital (or interest rate) for building materials. It can also be interpreted as a flow cost of construction (considering that poor households may not have access to financial markets): since informal housing units are evolving structures, households build them little by little in practice. As for public flood protection investments, we do not model private flood protection investments or slum upgrading, and as such we do not make the difference between a "complete" and an "incomplete" informal housing unit: we intend to prioritize such extension in future work.

Housing supply We focus on the housing supply per unit of available land. Since informal units cannot be built vertically, it is equal to one for $h = IS$ and $\mu(x)$ for $h = IB$. Moreover, since the supply of (standardized) public housing is exogenous, it makes no difference how such units are built and we abstract from modeling the housing supply for $h = FS$. We are left with the problem of formal private developers.

To simplify the optimization program compared to Pfeiffer *et al.* (2025), we assume that they produce housing with a Cobb-Douglas, and not a CES, technology. Given the very flat gradient of built density in Cape Town (implying an elasticity of substitution between land and capital that is close to one in a CES specification), we consider that this is a good enough approximation (also see Epple *et al.* (2010) and Combes *et al.* (2021)):

$$s_{FP}(k) = \kappa k^{1-a} \tag{3}$$

where κ is a scale factor, $k = \frac{K}{L_{FP}}$ is the endogenous amount of capital per unit of available land, $0 < a < 1$ is the land elasticity (or budget share), and $1 - a$ is the capital elasticity.

Formal private developers therefore maximize a profit function (per unit of available land) defined as:

$$\Pi(x,k) = R_{FP}(x)s_{FP}(k) - \left(\rho + \rho_{FP}^{struct}(x) + \delta\right)k - \delta P(x) \tag{4}$$

As mentioned before, developers buy land from absentee landlords. To do so, they contract an infinite debt that they repay at interest rate δ every period: this is to avoid time dependence in a static model, and is without loss of generality if we assume no arbitrage between owning and renting of raw land. Note that the price of a raw unit of land, $P(x)$, can be recovered as a function of (endogenous) housing market rent $R_{FP}(x)$ from a zero-profit condition ($P(x) = \frac{\kappa^{\frac{1}{a}} a(1-a)^{\frac{1-a}{a}}}{\delta(\rho+\delta)^{\frac{1-a}{a}}} R_{FP}(x)^{\frac{1}{a}}$). Then, developers may rent out a quantity $s_{FP}(k)$ of housing they build at rent $R_{FP}(x)$, but need to cover for the cost of capital k, again at rate δ. Additionally, since they own the structures, they need to cover for both the standard capital depreciation rate ρ, and the expected fraction of capital destroyed due to floods, $\rho_{FP}^{struct}(x)$.

4.2 Equilibrium dwelling size

Again, we focus on the formal private housing sector since dwelling size is fixed for $h = FS, IS, IB$. Maximizing utility (1) under constraint (2) implicitly defines the optimal housing consumption $Q^*(x,i)$ as a function of the endogenous utility level u for each income group i:

$$u = \left(\frac{\alpha \tilde{y}_i(x)}{1 + \gamma \rho_{FP}^{content}(x)}\right)^{\alpha} \frac{Q^*(x,i) - q_0}{(Q^*(x,i) - \alpha q_0)^{\alpha}} A(x) \tag{5}$$

By considering that developers do not rent housing units below a legal threshold $q_{min} > q_0$, we therefore define the equilibrium dwelling size for $h = FP$ as: $Q_{FP}(x,i,u) = max\left[q_{min}, Q^*(x, i \mid u)\right]$

4.3 Equilibrium market rent

Plugging back $Q_{FP}(x,i,u)$ into the first-order optimality condition for formal private households (not shown), we obtain the bid rent for a space unit of housing $h = FP$:

$$\psi_i^{FP}(x,u) = \frac{(1-\alpha)\tilde{y}_i(x)}{Q_{FP}(x,i,u) - \alpha q_0} \tag{6}$$

By doing the same for households living in informal housing, with fixed dwelling size q_I and building value v_I, we obtain the following bid rents for $h = IS, IB$:

$$\psi_i^{IS}(x,u) = \frac{1}{q_I}\left(\tilde{y}_i(x) - \left(\rho + \delta + \rho_{IS}^{struct}(x)\right) v_I - \left(1 + \gamma \rho_{IS}^{content}\right)\left[\frac{u}{(q_I - q_0)^{1-\alpha} A(x) B_{IS}(x)}\right]^{\frac{1}{\alpha}}\right) \tag{7}$$

$$\psi_i^{IB}(x,u) = \frac{1}{q_I}\left(\tilde{y}_i(x) - \left(\rho + \delta + \rho_{IB}^{struct}(x)\right) v_I - \left(1 + \gamma \rho_{IB}^{content}\right)\left[\frac{u}{(q_I - q_0)^{1-\alpha} A(x) B_{IB}(x)}\right]^{\frac{1}{\alpha}}\right) \tag{8}$$

Assuming that households bid their true willingness to pay and that there are no strategic interactions, housing is allocated to the highest bidding income group in each area where housing of a given type $h = FP, IS, IB$ is available. The upper envelope of bid rents therefore identifies the equilibrium market rent $R_h(x)$ across space. Finally, remember that the rent is exogenously taken as zero for $h = FS$.

4.4 Equilibrium housing supply

In the formal private sector, profit maximization of developers with respect to capital (per unit of land) in equation (4) defines the optimal quantity of invested capital. Plugging this value back into equation (3) yields:

$$s_{FP}(x) = \kappa^{\frac{1}{a}}\left(\frac{(1-a)R_{FP}(x)}{\rho + \rho_{FP}^{struct}(x) + \delta}\right)^{\frac{1-a}{a}} \tag{9}$$

In the informal backyard sector, utility maximization of (the poorest) households living in formal subsidized housing with respect to the fraction of backyard space that is rented out yields:

$$\mu(x) = \alpha\frac{q_{FS} - q_0}{Y} - (1-\alpha)\frac{\tilde{y}_1(x) - \left(\rho + \rho_{FS}^{struct}(x)\right) h_{FS}}{Y R_{IB}(x)} \tag{10}$$

4.5 Equilibrium population distribution

Finally, we divide the equilibrium housing supply (per unit of available land) by the dwelling size, and multiply it by the amount of available land to obtain the equilibrium number of households in each grid cell for each housing type. Then, we identify them as belonging to the highest bidding income group (for $h = FP, IS, IB$), and obtain:

$$N_i^h(x) = \frac{s_h(x) L_h(x)}{Q_h(x,i,u)} \tag{11}$$

where the numerator is exogenous and $i = 1$ for $h = FS$.

This is a direct consequence of housing market clearing. Note that labour market clearing is already embedded in the definition of $\tilde{y}_i(x)$ (see Section 5).

4.6 Closing the model

Following Sections 4.2-4.5, we therefore define an equilibrium as a set $\{u_i, R_h(x), s_h(x), N_i^h(x)\}$ for all i, h, and x where these functions are defined, and where the following constraints hold:

(i) $u_i^h(x) = u_i$ for all $x \in X_{\setminus FS}$ (set of locations occupied by households other than public housing beneficiaries) [*Spatial equilibrium*]: to ensure that there is no profitable deviation in equilibrium, all members of a given income group should be indifferent between available location-housing pairs (with the exception of public housing beneficiaries who all have a different utility level resulting from the random allocation of housing units that are more or less well located)

(ii) $P(x) \geq P_A$ for $x \in X_{FP}$ (set of locations occupied by formal private housing dwellers) and P_A is the price of raw agricultural land [*City-edge constraint*]: at the city fringe, absentee landlords must be indifferent between selling their land to a developer or engaging in agricultural activities, which endogenously defines city boundaries

(iii) $N_i = \sum_h \sum_x N_i^h(x)$ [*Population clearing*]: the city hosts all individuals in equilibrium

The numerical algorithm we use to solve for the equilibrium directly follows from this definition. Starting from arbitrary utility levels for each income group, with the exception of public housing beneficiaries (condition (i)), we sequentially solve for the quantities in Sections 4.2-4.5 and find the corresponding urban extent (condition (ii)). We then compute the error between the predicted populations $\sum_h \sum_x N_i^h(x)$ and the target populations N_i (condition (iii)). We update initial utility levels depending on the sign and size of the error terms: the larger the error, the more we increase utility, and conversely (note that $Q_h(x, i, u)$ is increasing in u in equation (11)). The process is iterated until the total absolute error falls below some predefined precision threshold.

This class of models corresponds to so-called "closed-city" models. Compared to "open-city" models where utilities are exogenous but total populations are endogenous, they do not allow the study of endogenous migration phenomena. In future work, we intend to leverage the dynamic structure of the model in Pfeiffer *et al.* (2025) to incorporate population growth scenarios from the City of Cape Town instead, along with a progressive extension of informal settlements (enabled by higher tolerance from the social planner) to host urban newcomers.

Finally, we do not formally prove that the equilibrium exists and is unique, but Pfeiffer *et al.* (2019) do it with a simpler framework. However, the fact that the algorithm converges, and that it does towards the same results for 250 simulations starting from a wide range of initial values, strongly suggests that the equilibrium does exist and is indeed unique.

5 Estimation

In this section, we cover the estimation procedure for the exogenous parameters and variables in the model. We refer the reader to Pfeiffer *et al.* (2025) for more detailed analyses of the estimation results (which slightly differ quantitatively, but not qualitatively) and general validation of the approach, as our focus in this paper is on the impact of flood risks more specifically.

5.1 Expected income net of commuting costs

We consider C employment locations, indexed by $c = 1, ..., C$, offering wage w_{ic} to members of income group i. The purpose of this subsection is to estimate wage w_{ic}, and deduct expected income net of commuting costs $\tilde{y}_{ic}$. Note that this quantity is estimated at baseline and does not change across counterfactuals. Our model should therefore be interpreted as a spatial equilibrium model of the housing market - not inclusive of the labour market - in which we will nest a workplace choice model (see below). We would like to assess how strong an assumption that is by looking at the effects of real flood events in future work.

Workplace choice model Given exogenous employment rates χ_i, households consider real income $y_{ic} = \chi_i w_{ic}$ when choosing job centers (and residential locations). Note that we consider households as representative individual workers. To commute between their residential and work locations, they further choose between M potential modes of transportation, denoted by m. For each mode m, residential location x, job center c, and income group i, households of type j face real commuting cost:

$$t_{mj}(x, c, w_{ic}) = \underbrace{\chi_i \left(\tau_m(x, c) + \delta_m(x, c) w_{ic}\right)}_{\overline{t_m}(x,c,w_{ic})} + \epsilon_{mxcij}$$

where $\tau_m(x, c)$ is the monetary transport cost and $\delta_m(x, c)$ is the opportunity cost fraction of time spent commuting.

ϵ_{mxcij} follows a Gumbel minimum distribution of mean 0 and scale parameter $\frac{1}{\lambda}$. It captures the fact that, all else equal, households may have idiosyncratic preferences that rationalize the coexistence of different individual choices within a given income group in equilibrium.

Commuters pick the transport mode that minimizes their real commuting cost. Due to the properties of the Gumbel minimum distribution, this yields:

$$\underset{m}{min} \left(t_{mj}(x, c, w_{ic})\right) = -\frac{1}{\lambda} log \left(\sum_{m=1}^{M} exp \left[-\lambda \overline{t_m}(x, c, w_{ic})\right] \right) + \eta_{xcij}$$

where η_{xcij} also follows a Gumbel minimum distribution with same parameters.

Households therefore still have idiosyncratic preferences for residential-work location pairs once modal choice is accounted for. Note that we will check ex post that the above quantity is well defined for the estimated value of λ.

For a given residential location x, households therefore choose a workplace c that maximizes their real income net of commuting costs, solving the program: $\underset{c}{max}\left[y_{ic} - \underset{m}{min}\left(t_{mj}(x, c, w_{ic})\right)\right]$. Since this corresponds to the latent variable formulation of a multinomial logit model, the expected income net of commuting costs $\tilde{y}_i(x) \equiv \mathbb{E}\left[y_{ic} - \underset{m}{min}\left(t_{mj}(x, c, w_{ic})\right)\right]$ that enters the main housing choice model can be defined as:

$$\tilde{y}_i(x) = \sum_{c=1}^{C} \pi_{c|ix}\left[y_{ic} + \frac{1}{\lambda}\log\left(\sum_{m=1}^{M}\exp\left[-\lambda\overline{t_m}(x, c, w_{ic})\right]\right)\right]$$

with:

$$\pi_{c|ix} = \frac{\exp\left[\lambda y_{ic} + \log\left(\sum\limits_{m=1}^{M}\exp\left[-\lambda\overline{t_m}(x, c, w_{ic})\right]\right)\right]}{\sum_{k=1}^{C}\exp\left[\lambda y_{ik} + \log\left(\sum\limits_{m=1}^{M}\exp\left[-\lambda\overline{t_m}(x, c, w_{ic})\right]\right)\right]}$$

Commuting cost calibration Based on the 2011 National Census, we consider employment rates $\chi_{i=1,...,4} = [0.57, 0.97, 0.96, 0.97]$.

We also assume that the monetary transport cost takes functional form $\tau_m(x, c) = T(F_m + d_{xc}V_m)$, where F_m and V_m are mode-specific fixed and variable cost components, and d_{xc} is the distance (in km) between points x and c (from Cape Town's transport model). In the model, we consider $C = 185$ main job centers. T is a constant equal to the number of trips per year, that we set to 470.

We consider five transportation modes that are prevalent in the context of Cape Town: train, bus, minibus/taxi, car, and walking. Walking is free. For the three public transportation modes, we estimate the fixed and variable cost components by regressing transport cost statistics on residence-workplace distances taken from Roux & Yolandi (2013). Considering estimates for the average price of a car, and that materials roughly account for half of this value, we apply capital depreciation rate ρ to this cost component to obtain the yearly vehicle fixed cost, that we divide by T. For the vehicle variable cost, we consider fuel prices and energy efficiency data from the International Energy Agency to obtain a price per km at baseline year. Table 1 summarizes the values we find for each mode:

Table 1: Summary table of monetary transport cost parameters

Mode	F_m	V_m
Train	4.48	0.164
Bus	4.32	0.785
Minibus/taxi	6.24	0.522
Car	10.00	1.157

As for the opportunity cost fraction of time spent commuting, $\delta_m(x, c)$, we assume that it is equal to the fraction of working time spent commuting, or that the opportunity cost of not working is equal to one. Here, we consider the labour supply elasticity as perfectly inelastic (8 hours a day), and rule out the possibility that workers may commute out of their leisure time. The time spent commuting is directly given by Cape Town's transport model, except for walking, which we assume to have a 4km/h speed.

Estimation of λ and w_{ic} From the workplace choice model, we can derive the expected number of residents of income group i choosing to work in c, denoted W_{ic}, provided that we know the number of residents of income group i with their residence in x, denoted $N_i(x)$, in all locations x. This yields:

$$W_{ic} = \chi_i \sum_x \pi_{c|ix} N_i(x)$$

Note that summing this relation over job centers c yields a labour market clearing condition.

Since the values for W_{ic} and $N_i(x)$ are respectively given by Cape Town's transport model and the National Census, we first solve the above equation for w_{ic}, for discrete values of parameters λ. This is done numerically by starting with average values $\overline{w_i}$ from the census for w_{ic} in the right-hand side, and updating them iteratively until the target population is reached on the left-hand side. Then, we pick the $\{\lambda, w_{ic}\}$ pair that best fits the aggregate distribution of residence-workplace distances from Cape Town's Transport Survey: we obtain $\lambda = 13.96$.

Going back to the workplace choice model, we can now compute the value of expected income net of commuting costs $\tilde{y_i}(x)$.

5.2 Housing production function parameters

By plugging the value of formal private housing supply (per unit of available land) from equation (11) in the left-hand side of equation (9), and considering that $R_{FP}(x) = \frac{(\delta P(x))^a (\rho+\delta)^{1-a}}{\kappa a^a (1-a)^{1-a}}$ (zero-profit condition), we obtain the following log-linear relation, that we estimate at the "sub-place" (census tract) level s using the property transaction data:

$$log(N_s^{FP}) = \gamma_1 + \gamma_2 log(P_s) + \gamma_3 log(Q_s) + \gamma_4 log(L_s^{FP}) + \epsilon_s$$

where $\gamma_1 = log\left(\kappa(\frac{1-a}{a})^{1-a}\right)$, $\gamma_2 = 1-a$, $\gamma_3 = -1$, and $\gamma_4 = 1$.

As this theoretical relation only holds for developed formal private housing, we exclude sub-places in the bottom quintile of property prices (not necessarily representative of competitive markers), where more than 5% of households are reported to live in informal housing, or which we classify as rural (large areas in the highest surface quantile, where less than 60% of the land can be developed, or located more than 40km away from the CBD). We also exclude the poorest income group who may benefit from public housing options. Table 2 shows the results.

The fact that the estimated values for $\widehat{\gamma_3}$ and $\widehat{\gamma_4}$ are reasonably close to -1 and 1, respectively, suggests that the relation is indeed well identified. Solving for a and κ with the estimated values for $\widehat{\gamma_2}$ and $\widehat{\gamma_1}$, respectively, yields $a = 0.758$ and $\kappa = 0.031$.

Table 2: Estimated coefficients from log-linear regression on property transaction data

$\widehat{\gamma_1}$	$\widehat{\gamma_2}$	$\widehat{\gamma_3}$	$\widehat{\gamma_4}$
-3.763	0.242	-0.895	0.995
(0.981)	(0.069)	(0.094)	(0.070)

5.3 Utility function parameters

Stone-Geary specification We use a simplified calibration procedure compared to Pfeiffer *et al.* (2025), that we deem more robust. We set basic need in housing $q_0 = 4m^2$ to reflect the very minimum size of informal units from Rice *et al.* (2023). Then, we set the income elasticity of housing expenditure $1 - \alpha = 0.25$ following Finlay & Williams (2022), who estimate this term for more general non-homothetic preferences. As a matter of fact, these values happen to be very close from the ones in Pfeiffer *et al.* (2025).

Amenity index As for the estimation of the amenity index $A(x)$, we leverage property price data for formal private housing and information on exogenous amenities from the City of Cape Town, defined at the sub-place (census tract) level s. Let us define the observed amenity index as:

$$A_s = \prod_n (a_{n,s})^{\vartheta_n} \epsilon_{A,s}$$

where $a_{n,s}$ are exogenous amenity dummies from the data, ϑ_n are their respective elasticities, and $\epsilon_{A,s}$ is an error term.

Taking housing rents from the data and inverting equation (1) for formal private dwellers (essentially the two richest income groups) also yield the amenity index A_s as a function of the dominant income group's utility level $u_{i(s)}$. We can therefore estimate the log-linearization of the above equation for discrete values of $u_{i(s)}$. We pick the value set that minimizes the error $\epsilon_{A,s}$, and use the estimated ϑ_n to recover the predicted value of $A(x) = \prod_n (a_{n,x})^{\vartheta_n}$, at the grid cell level. Table 3 shows the corresponding regression results.

Informal disamenity index Finally, we recover the disamenity indices $B_{IS}(x)$ and $B_{IB}(x)$ by model inversion. To do so, we start by solving the full model using the constant terms $\overline{B_{IS}}$ and $\overline{B_{IB}}$ from Pfeiffer *et al.* (2025). Then, we update the values in each location x depending on the prediction error on local populations $N^{IS}(x)$ and $N^{IB}(x)$. We stop after a fixed number of iterations.

5.4 Externally calibrated parameters

Table 4 summarizes the values and sources for additional model parameters that are externally calibrated.

The first panel deals with aggregate dwelling size parameters provided by the City of Cape Town. q_{min} is a legal requirement, whereas the other values are estimates from the field. The

Table 3: Results of the log regression of predicted amenity index on exogenous amenities

	$log(A_s)$
Prox. to district park (¡1km)	-0.051
	(0.043)
Prox. to ocean (¡2km)	0.063
	(0.041)
Prox. to ocean (¡4km)	0.011
	(0.046)
Prox. to urban heritage site (¡2km)	0.185
	(0.052)
Within airport noise cone	-0.007
	(0.067)
Slope (betwen 1 and 5%)	0.144
	(0.034)
Slope (¿5%)	0.121
	(0.049)
Prox. to biosphere reserve (¡2km)	0.098
	(0.038)
Prox. to train station (¡2km)	0.039
	(0.035)
Constant	-0.458
	(0.038)
Obs.	307
R^2	0.160
F-stat	6.268
D.f.	297

Table 4: Summary table of externally calibrated parameters

Parameter	Value	Source
q_{min}	30 (m^2)	City of Cape Town
q_{FS}	110 (m^2)	City of Cape Town
Y	70 (m^2)	City of Cape Town
q_I	14 (m^2)	City of Cape Town
v_{FS}	126,000 (ZAR)	Expert assessment (PDG)
v_I	3,000 (ZAR)	Expert assessment (PDG)
γ	0.27	Quantec (HH budget breakdown)
P_A	807.2 (ZAR)	Property transaction data
ρ	0.025	Viguié *et al.* (2014)
δ	0.038	World Development Indicator database (2016)

fact that they are fixed values reflects the relative standardization of RDP/BNG public housing schemes on one side, and informal construction technologies on the other. Although these are simplifications, we consider them as good first-order approximations.

The second panel deals with parameters relative to flood damages. The accounting value of formal subsidized and informal (both settlements and backyards) buildings is based on expert assessments of the material costs, along with surveys of construction technologies used in the field. The share of composite good that is vulnerable to floods corresponds to the average budget share households spend on durable and semi-durable goods, that are not consumed immediately and are kept within the house.

The third panel deals with the remaining parameters. The agricultural price corresponds to the highest decile in the property price data when selecting rural areas only (see definition below). The capital depreciation rate is 2.5 times higher than the one used by Viguié *et al.* (2014) for Paris (France), so as to account for the overall lower construction quality in Cape Town. Finally, the interest rate corresponds to the 4-year average up to baseline year (2011) in the World Development Indicator database, so as to smooth its volatility.

6 Simulations

In what follows, we run our benchmark model and conduct two comparative statics. In the first one, we compare our benchmark to a version of the model where agents do not anticipate flood risks. They therefore make their housing and location decisions ex ante, as in Pfeiffer *et al.* (2025), only to realize flood damages ex post. Because this is not an equilibrium outcome, utility levels cannot be directly compared between the two output sets. Instead, we consider damage shares of income as a proxy of welfare losses due to floods.

The comparison between the two models yields the theoretical policy impact of going from a polar case where agents have no information about flood risks to another polar case where they have perfect information. Avner *et al.* (2019) and Liotta *et al.* (2023a) show that the latter is equivalent to complete market- or self-insurance. The reality of the current situation and of policy effectiveness probably lies in between, and our results should therefore be taken as an upper bound on policy impacts. We intend to more precisely calibrate agents' imperfect foresight and behaviour updating following information shocks in future work (Bakkensen & Ma, 2020; Kousky *et al.*, 2020; Hino & Burke, 2021).

In the second comparative static, we compare our benchmark to a version of the model where flood risks are updated to account for climate change. Since we do not currently allow for protection investments, these results should also be taken as an upper bound for the effect of climate change on spatial inequalities. We still see our simulations as a strong contribution to the existing flood damage literature, given the key local housing conditions that are featured in our approach.

6.1 Information

Aggregate damages We plot the distribution of aggregate annual damages across housing and damage types in Figure 4, comparing our two polar cases, for each flood type.

Figure 4: Aggregate flood damage estimates across flood types w/ and w/o/ anticipation

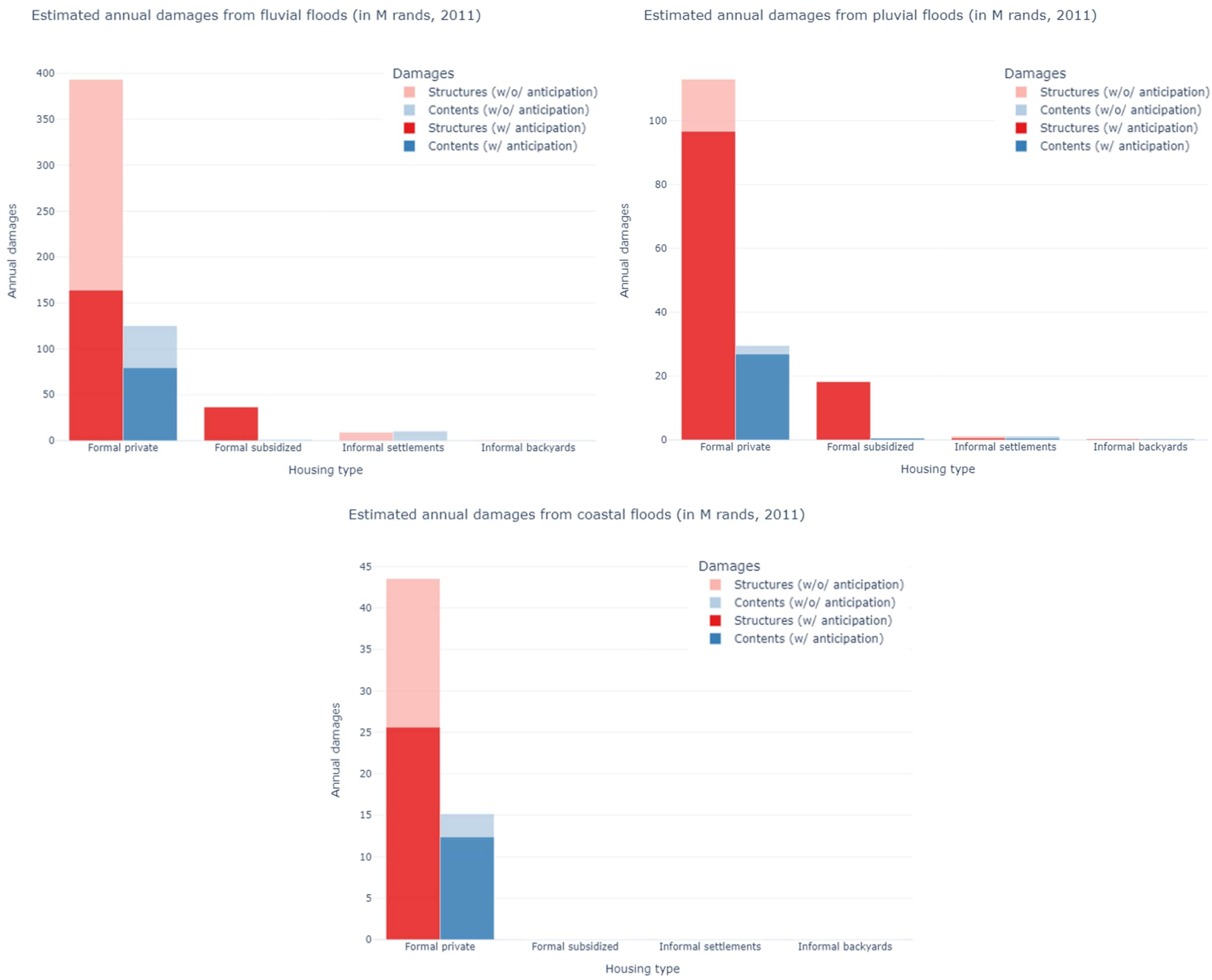

Several comments are in order. First, damages in formal housing are consistently larger than in informal housing, although the latter is more vulnerable to flooding (due to building materials used and locations of informal settlements), and damages to structures also tend to outweigh damages to contents. This is because the replacement cost of informal settlements and backyard structures is based on construction costs that are fairly low. Formal private housing, on the other hand, is built according to higher and more costly standards, and will typically use land more intensively in attractive locations such that buildings can be tall and capital-intensive. The replacement cost of formal subsidized housing structures lies somewhere in between. Finally, the population living in formal private housing essentially belongs to the two richest income groups. Their higher amount of income available for consumption explains the relative importance of content damages in this category.

Second, damages are higher in the no-anticipation case than in the perfect-anticipation case. This is to be expected. Anticipation also seems to play a relatively more important role in avoiding damages in the formal private housing sector. This is because it is the least constrained of the housing submarkets, either in terms of available locations, or restrictions on supply and demand. Moreover, anticipation plays a contrasted role across flood types. Again, this can be interpreted in terms of existing constraints: pluvial flood zones are typically more dispersed than fluvial or coastal flood zones, hence are harder to avoid on the extensive margin of adaptation (location). Independently, coastal flood zones are typically more attractive, hence a higher willingness to stay there and adapt on the intensive margin (consumption).

Third, damages also significantly vary in magnitude across flood types. Table 5 summarizes aggregate damage estimates per flood type in our two polar cases, with values converted between 2011 ZAR and 2021 USD using an inflation rate of 64% and an exchange rate of 14.78 ZAR/USD. Total damages are smaller than the sum of individual categories as we avoid double counting when pluvial and fluvial flood zones overlap.

Table 5: Summary table of aggregate damage estimates w/ and w/o/ anticipation

	Perfect information	No anticipation
Fluvial	280M (ZAR, 2011)	470M (ZAR, 2011)
	31M (USD, 2021)	*63M (USD, 2021)*
Pluvial	145M (ZAR, 2011)	165M (ZAR, 2011)
	16M (USD, 2021)	*18M (USD, 2021)*
Coastal	50M (ZAR, 2011)	75M (ZAR, 2011)
	6M (USD, 2021)	*8M (USD, 2021)*
Total	448M (ZAR, 2011)	750M (ZAR, 2011)
	49M (USD, 2021)	*83M (USD, 2021)*

For comparison, Gonzales *et al.* (2023) estimate aggregate annual flood damages in Cape Town at around 16M USD (at 2021 values). The key difference between our results lies in the way the replacement cost of vulnerable assets is determined. In their paper, a standard capital value is calibrated and yields flood damages based on depth-damage conversions. In our paper, the capital value of buildings is an endogenous outcome that can quickly rise in attractive areas, and we also take housing contents into consideration. In fact, our total estimate for the capital value of the city is in line with that of the authors. The reason why we find higher damages therefore boils down to a composition effect, as we are able to simulate how capital gets distributed across space, notably in flood-prone zones.

At any rate, our paper shows that material flood damages are high (potentially higher than previously thought), and that information/insurance is a key policy lever to mitigate them, with a reduction potential of up to 41%.

Absolute damage distribution Figure 5 shows how flood damages spread out across the city in the no-anticipation case, and the absolute change this corresponds to compared to the benchmark perfect-information case. The highest damage values concentrate in populated areas along rivers near the city center and to the north, where some important job centers are located and rent is still relatively high. These are also areas where values change the most compared to the benchmark case, suggesting an important adaptation of households on the extensive margin following an information shock.

Figure 5: Spatial absolute flood damage estimates w/ and w/o/ anticipation (ZAR, 2011)

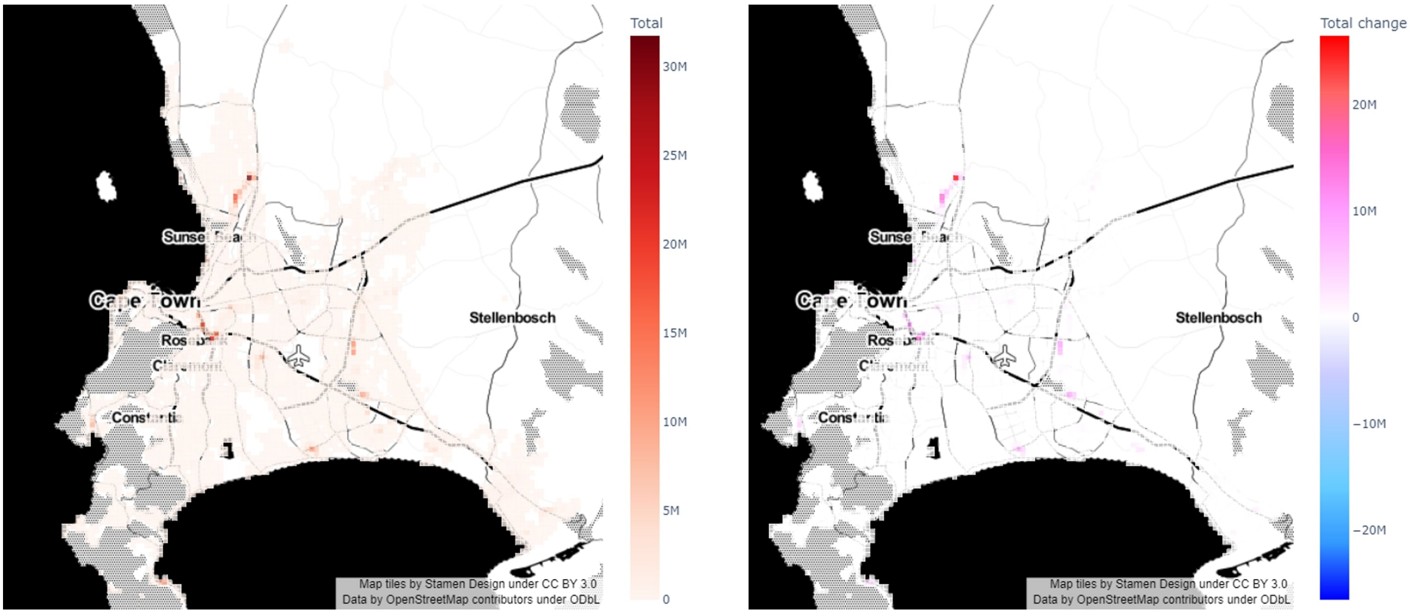

Note: The map on the left shows the values under no flood risk anticipation. The map on the right shows the change (in absolute terms) it represents compared to baseline (perfect anticipation).

In relative damage terms (as a share of expected income net of commuting costs, henceforth net income), values would appear to be higher in the north than in the city center, and even more to the east, where poorer households live. As households of different types move across locations in the two polar cases, it is not possible to properly estimate the changes in relative damages at the grid-cell level. Instead, we now turn to their aggregate distribution per income group to see how flood damages translate into welfare losses.

Relative damage distribution Figure 6 plots the aggregate distribution of relative flood damages per income group. Since there is a high mass of households who do not live in flood-prone areas, the graphs only consider the subpopulation living in areas with a positive risk of floods. In the interest of space, we only show results for fluvial flood risks (since they are the most impactful in households' adaptive behaviour).

We see that richer households are less likely to live in flood-prone zones, even in the no-anticipation case: this is because they typically are low-amenity areas located far from job centers. Interestingly, conditional on flood exposure, the tail of relative damage distributions does not necessarily become thinner as income increases in the perfect-information case. This is because, as marginal utility decreases with income, richer households become comparatively less sensitive to flood damages.

As a side note, the very high relative damage values for the poorest income group do not only

Figure 6: Relative fluvial flood damage distribution by income group w/ and w/o/ anticipation

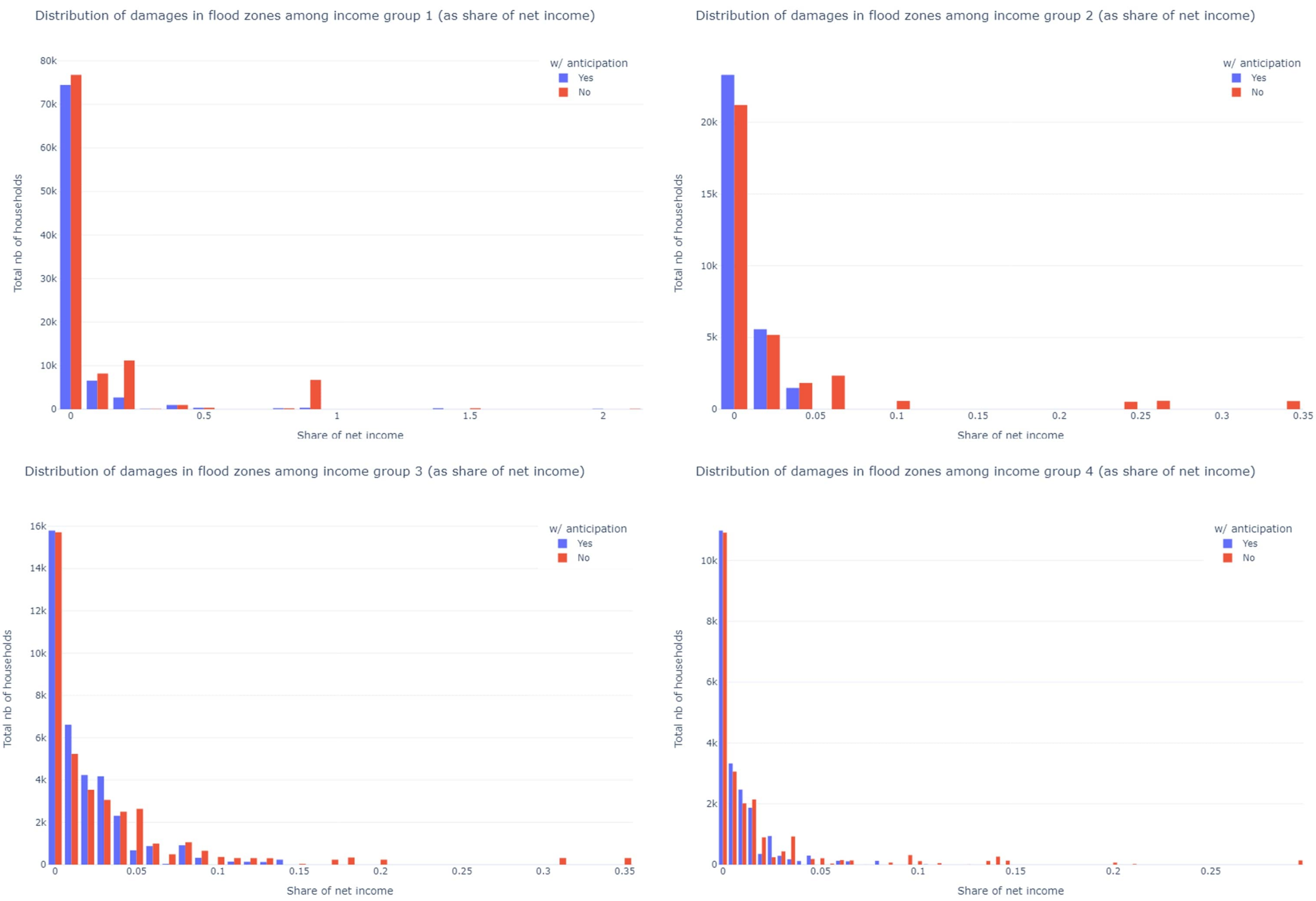

relate to their low income levels, but also to the fact that replacement costs of formal subsidized housing are very high (compared with informal housing): in cases where this option becomes unsustainable (or simply less valuable than informal options), the local government would have to bail public housing beneficiaries out.

To visualize more clearly the adaptation response, Table 6 summarizes average relative damage estimates per income group. Here is the bottom line. In our simulations, the total income gain generated by the information shock is equal to more than 4% for 20% of the total population (that is initially exposed to flood risks). This is the result of an adaptive behaviour on both the extensive (households moving to areas with lower flood risks, potentially leaving flood-prone zones entirely) and the intensive (households trading off goods and housing consumption) margins.

When analyzing the heterogeneity by income group, we show that the poorest income group (that is crowded out of the formal private sector) makes up roughly half of the total exposed population. Households are also more likely to live in flood-prone areas conditional on their belonging to this group, and have the largest share of income destroyed by floods. They therefore strand to gain the most from the policy, with total income gains rising to 7% for this group. As we saw, this is in spite of their option set being more constrained, which leaves room for even

Table 6: Summary table of relative damage estimates w/ and w/o/ anticipation

	Perfect information	No anticipation
Inc. group 1		
Inc. destroyed	3.37%	9.83%
Exposed pop.	87,582	104,723
Group share	22%	26%
Tot. inc. gain	*+7.01%*	
Inc. group 2		
Inc. destroyed	0.60%	2.57%
Exposed pop.	30,363	32,789
Group share	18%	19%
Tot. inc. gain	*+2.01%*	
Inc. group 3		
Inc. destroyed	1.79%	3.08%
Exposed pop.	36,593	38,620
Group share	12%	13%
Tot. inc. gain	*+1.38%*	
Inc. group 4		
Inc. destroyed	0.76%	1.59%
Exposed pop.	21,192	22,624
Group share	13%	14%
Tot. inc. gain	*+0.88%*	
All		
Inc. destroyed	2.25%	6.39%
Exposed pop.	175,730	198,656
Group share	17%	19%
Tot. inc. gain	*+4.40%*	

further gains under more accommodating housing policies.

Flood damages and policy responses therefore appear to be high, not only in absolute but also in relative terms, even though the household and housing types that are the most affected are not the same in the two cases. We now give more details on the form adaptation takes in practice.

Population moves: the extensive margin Figure 7 shows the spatial population distribution in the non-anticipation case, and the change it corresponds to (in absolute terms) compared to the benchmark perfect-information case. As already mentioned, the population density is the highest in informal settlement areas in the east (which exist alongside formal private housing units). Note that public housing (hence informal backyard) units tend to be located in the same zones. Interestingly, these are also the areas where there appears to be the most moves between the two polar cases: poor households appear to be relatively mobile, even though they do not seem to move far from their original location.

Figure 7: Spatial population distribution w/ and w/o/ anticipation

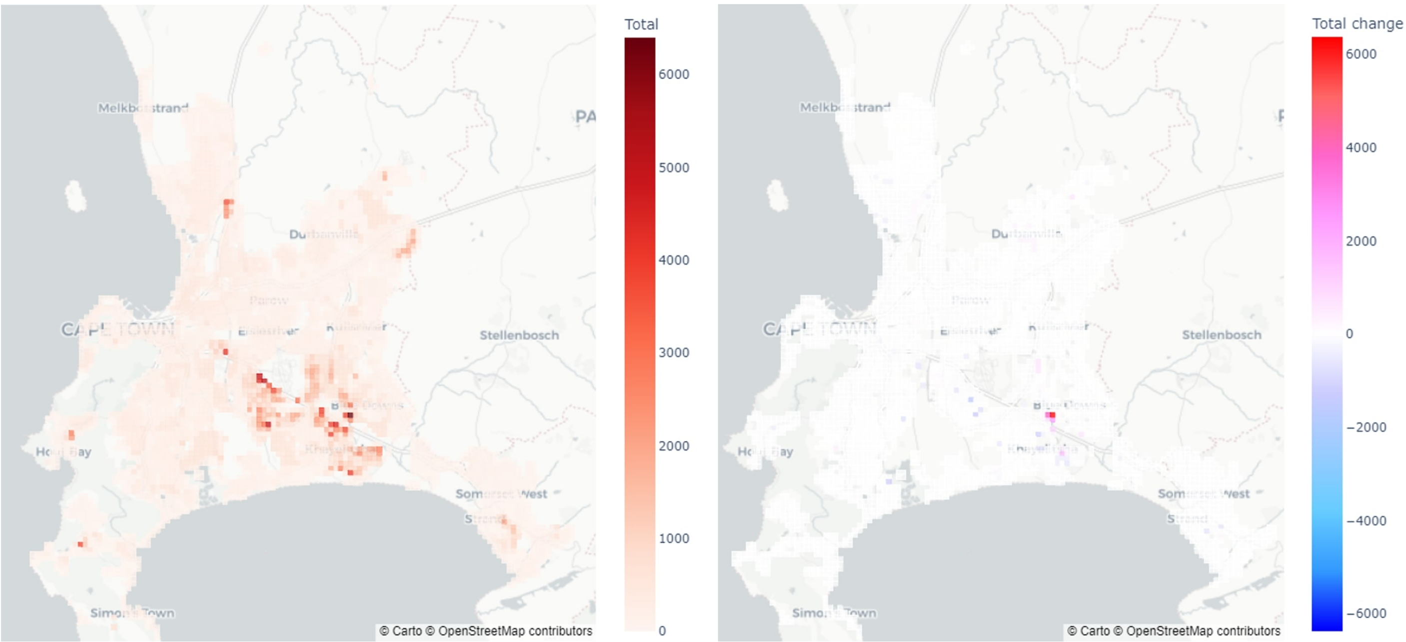

Note: The map on the left shows the values under no flood risk anticipation. The map on the right shows the change (in absolute terms) it represents compared to baseline (perfect anticipation).

Changes in rents: the intensive margin Figure 8 shows the spatial changes in rents (in absolute terms) across the three endogenous housing submarkets in the model. As could be expected, rents generally increase with population as they both capture the willingness to pay of households across the two polar cases. Interestingly, they also move in places where there are no strong population changes, and even more so where we expect relatively poor households to live. This suggests that adaptation also occurs on the intensive margin, with households demanding lower rents to be compensated for the cost of living in flood-prone zones (or willing to pay more not to be crowded out of safe places). This effect is stronger for vulnerable populations who are more sensitive to changes in income.

Figure 8: Absolute change in spatial rent (rands/m²) per housing type under no anticipation

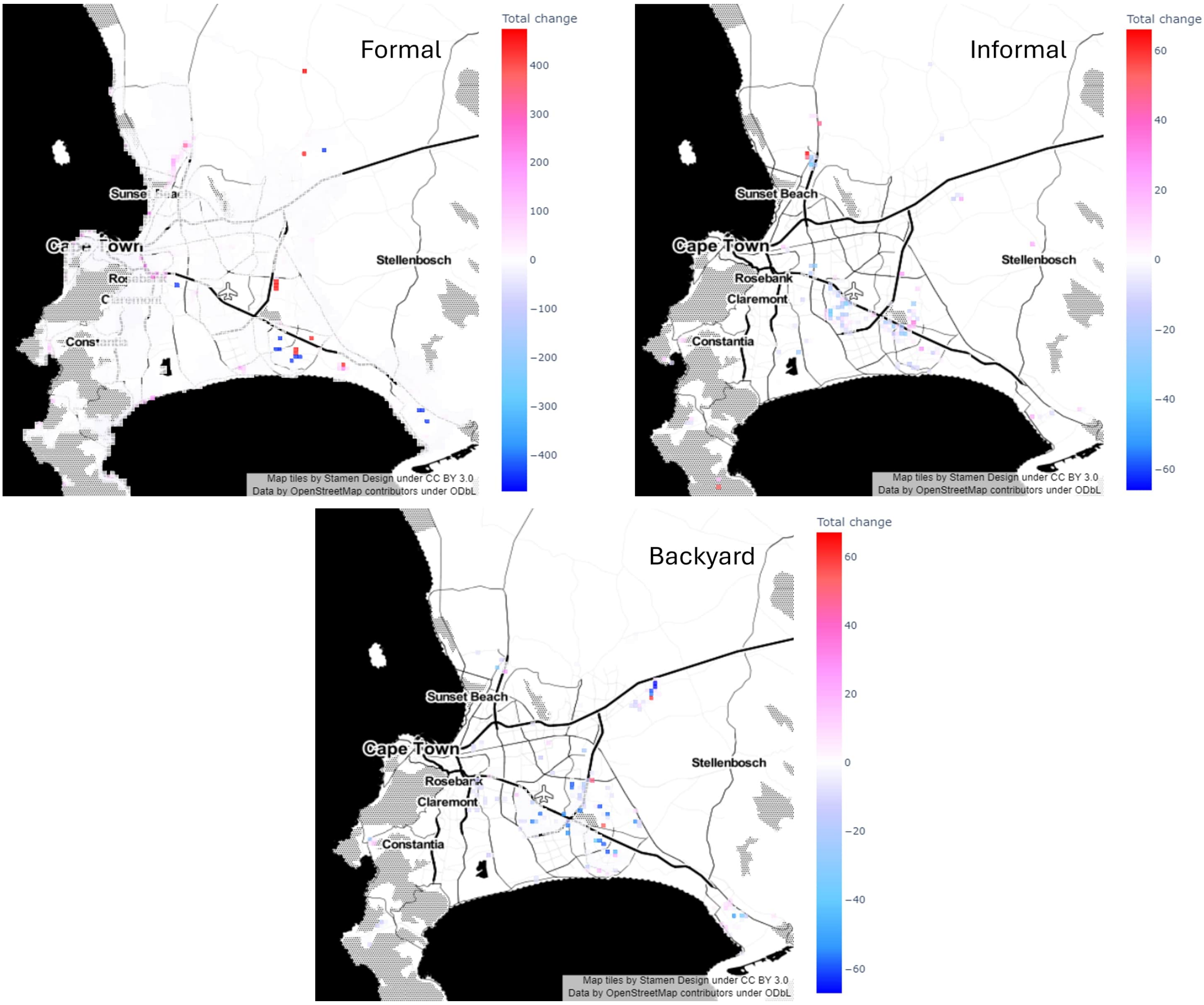

All in all, poor households seem to be reactive to the information/insurance shock, with a response on the extensive margin that allows them to reduce their exposure to flood risks, and a response on the intensive margin that allows them to be partly compensated through changes in rents when they are not able or willing to move away. Let us now see what kind of behaviour they adopt when it comes to climate change.

6.2 Climate change

Aggregate damages As before, we start by plotting aggregate damages per flood type across our scenarios, this time with and without climate change, in Figure 9. Let us observe that the largest change now occurs for pluvial flood risks, and not fluvial ones. The explanation is the same as before: since pluvial flood zones are more spread out, climate change there is harder to avoid. Again, coastal flood zones fall in between as they typically are high-value areas where households prefer to adapt their housing consumption rather than their location choice.

Otherwise, the pattern is similar to the previous comparative static, with substantial increases in flood damages when introducing climate change.

Figure 9: Aggregate flood damage estimates across flood types w/ and w/o/ climate change

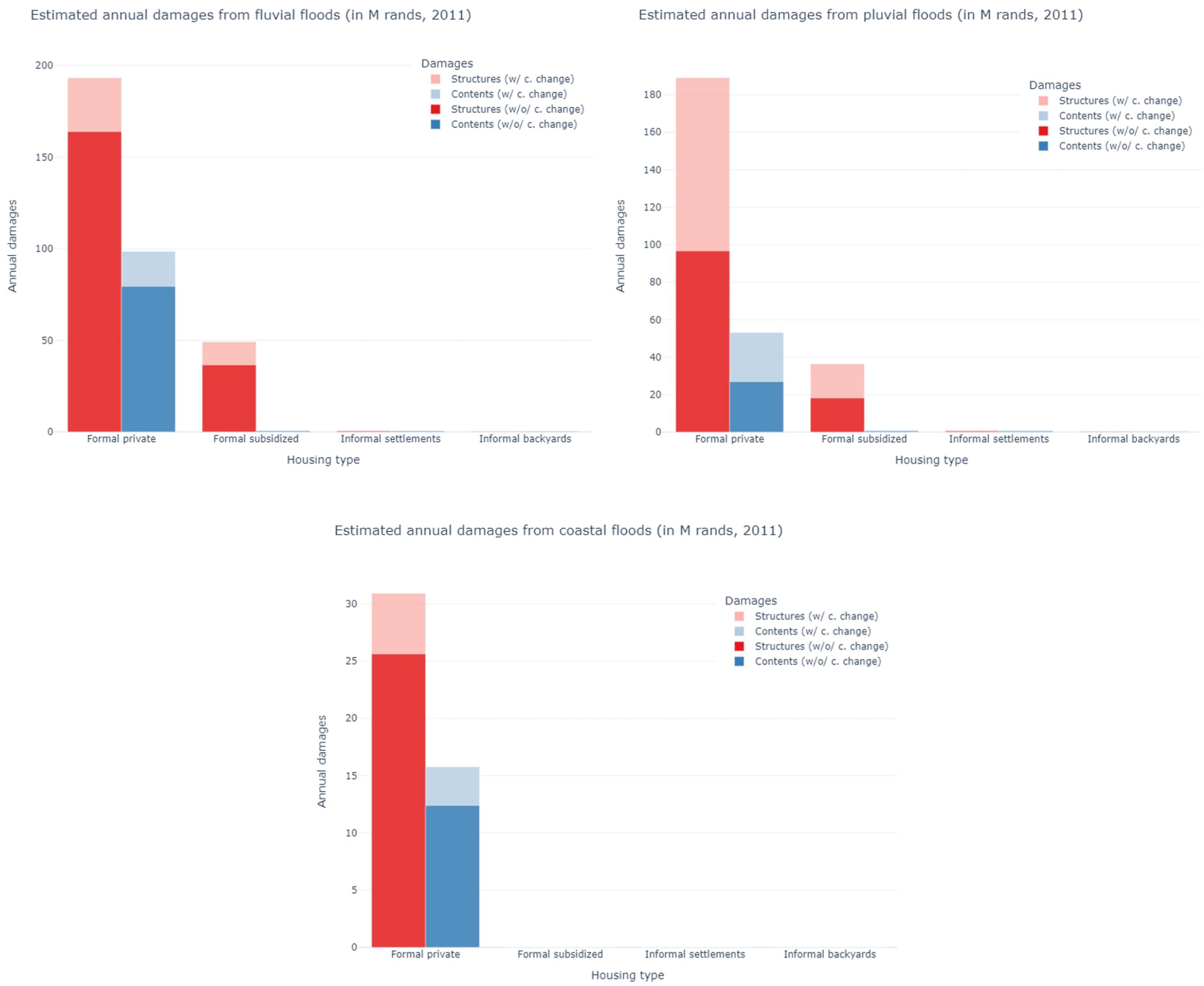

We do not reproduce the aggregate damage estimate table whose primary function was to compare our results with those of Gonzales *et al.* (2023), who do not consider climate change in their model.

Absolute damage distribution Figure 10 reproduces the spatial distribution of absolute damages in our benchmark case, and shows how they increase when taking climate change into account. We observe that the change across scenarios is more widely spread (but also smaller per unit of land) than in the previous comparative static (as pluvial flood risks are more spread out, but also less severe than fluvial ones).

Relative damage distribution Contrary to the previous comparative static, both scenarios are now equilibrium outcomes (ex post flood damages). We can therefore directly compare the utility levels of each income group (assuming cardinal utilities) to assess the welfare impacts

Figure 10: Spatial absolute flood damage estimates w/ and w/o/ climate change (ZAR, 2011)

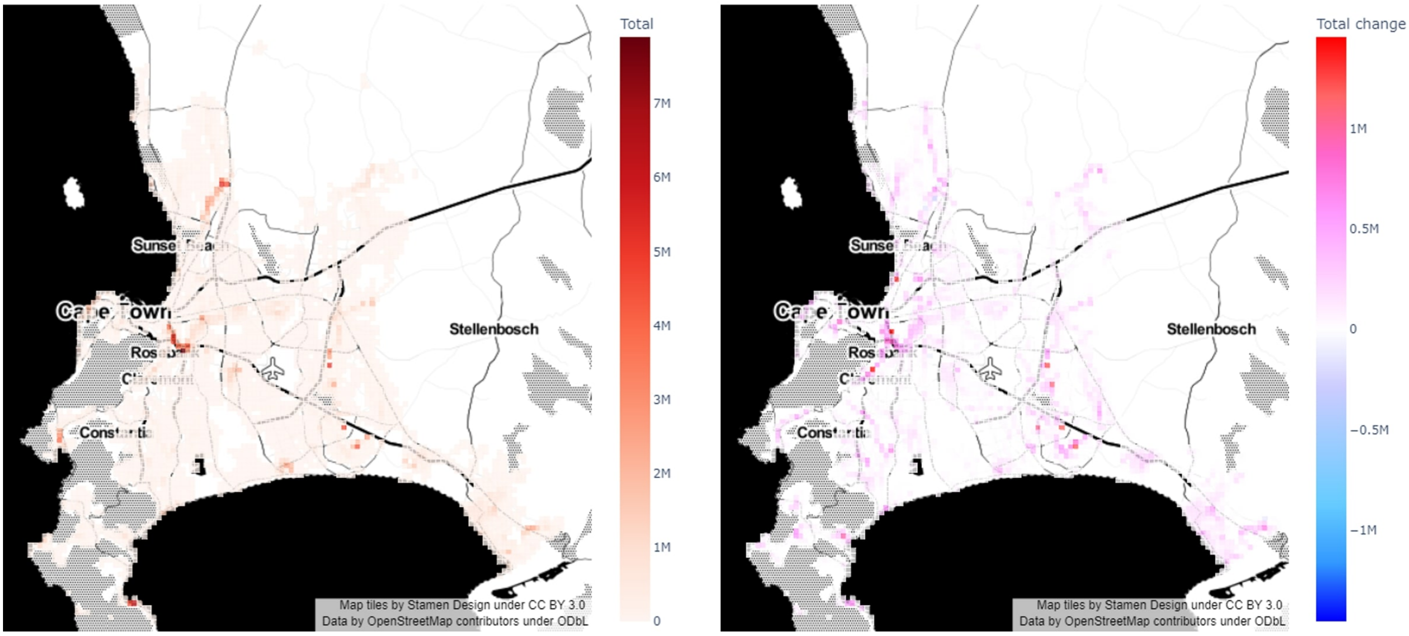

Note: The map on the left shows the values at baseline (perfect anticipation). The map on the right shows the change (in absolute terms) when considering climate change.

of climate change in the model. We find very marginal (negative) effects: the poorest income group is almost not affected, the second poorest is 0.07% worse off, and the two richest are 0.05% worse off. We argue that this is mostly due to an effective adaptation of households with respect to fluvial flood risks, and lower pluvial flood risks in comparison.

Note that such outcomes correspond to a long-term static equilibrium where the housing market has completely absorbed the effect of climate change, and where exposed and non-exposed households have become indifferent conditional on their income group. This says nothing of the adjustment mechanisms in a dynamic setting. We therefore now turn, as before, to the relative damage distribution per income group to focus on direct losses households are faced with before rents adjust (but after potential population moves). Results are shown in Figure 11 for pluvial flood risks, since they are now the most impactful flood type across the two scenarios.

Compared to fluvial flood risks, there are more exposed households, and the distribution tails are typically thinner and shorter. As expected, we see exposure shifting from low-damage brackets to high-damage brackets when introducing climate change. Table 7 summarizes the results. As before, the poorest income group is the most affected, and this time stands to lose the most from the change. Overall, we estimate the relative damages from climate change to roughly 0.3% of net income for 90% of the total population. Assuming the same exposed population baseline as in the first comparative static, this would correspond to a loss of 1.7%, which is less important in absolute terms but not negligible.

Households therefore appear to be less able or willing to adapt to the consequences of climate change regarding pluvial, as opposed to fluvial, flood risks. Let us now turn to population moves

Table 7: Summary table of relative damage estimates under climate change

	Business as usual	Climate change
Inc. group 1		
Inc. destroyed	0.67%	1.34%
Exposed pop.	366,265	364,492
Group share	92%	92%
Tot. inc. loss		*-0.67%*
Inc. group 2		
Inc. destroyed	0.12%	0.23%
Exposed pop.	166,655	166,511
Group share	97%	97%
Tot. inc. loss		*-0.12%*
Inc. group 3		
Inc. destroyed	0.10%	0.20%
Exposed pop.	270,802	270,786
Group share	91%	91%
Tot. inc. loss		*-0.10%*
Inc. group 4		
Inc. destroyed	0.07%	0.13%
Exposed pop.	128,747	128,642
Group share	79%	79%
Tot. inc. loss		*-0.07%*
All		
Inc. destroyed	0.32%	0.64%
Exposed pop.	932,469	930,431
Group share	0.91%	0.90%
Tot. inc. loss		*-0.32%*

Figure 11: Relative pluvial flood damage distribution by income group under climate change

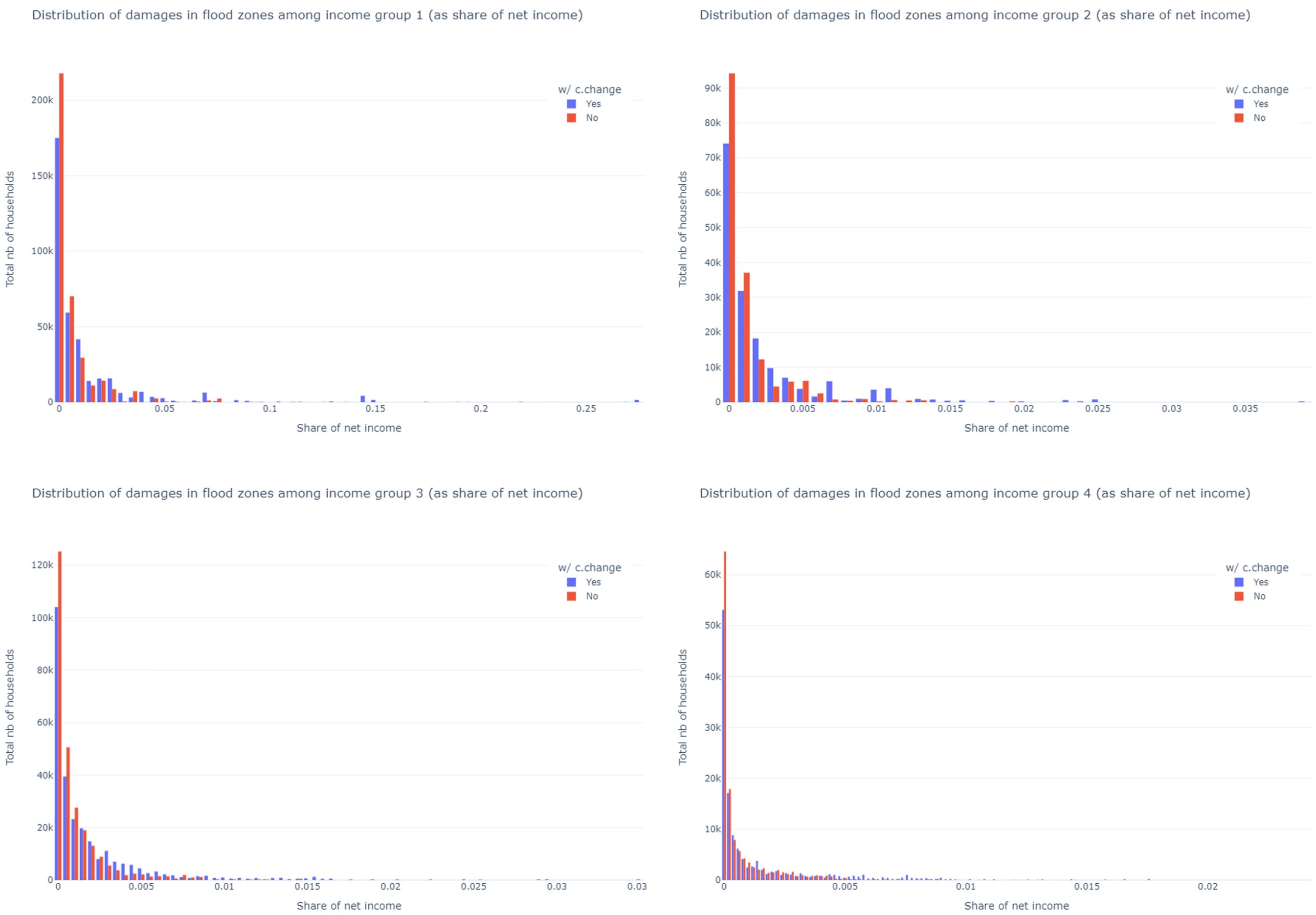

to assess their spatial adaptation strategies.

Population moves: the extensive margin Figure 12 shows the spatial population distribution at baseline, and how it evolves following the climate change shock. The pattern is similar to that of the first comparative statistic as households are again avoiding risks in fluvial flood zones, which explains why the increase in damages is limited in this category.

Changes in rents: the intensive margin Figure 13 plots the spatial evolution of rents across the three endogenous housing submarkets in our model. Again, there seems to be adjustments even when households do not change locations, reflecting their lower willingness to pay for exposed housing: contrary to the previous comparative static, rents mostly fall across the city, with very few rent increases in equilibrium. It is also worth noting that most of the changes are concentrated in informal housing, which is further exposed to pluvial floods compared to formal housing, due to the simulated absence of drainage systems. Such adjustments explain why the fall in utility levels is weaker than the fall in flood damages, especially for the poorest income group.

All in all, households seem to be responsive to the increase in flood risks due to climate change,

Figure 12: Spatial population distribution w/ and w/o/ climate change

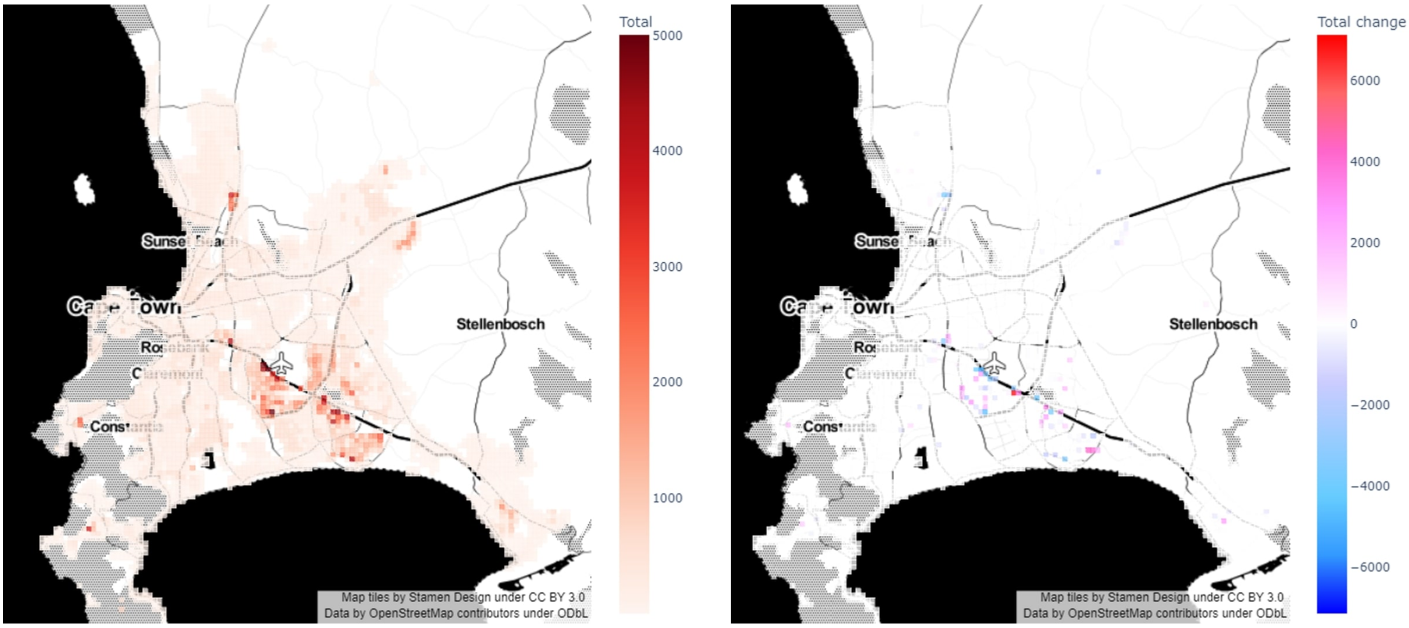

Note: The map on the left shows the values at baseline (perfect anticipation). The map on the right shows the change (in absolute terms) when considering climate change.

but such adaptation at the individual level hides substantial economic damages at the aggregate level.

7 Conclusion

In this paper, we presented a realistic urban simulation model for low- and middle-income countries, featuring income heterogeneity and informal housing. The key novelty is that it also features material damages from three types of flood risks (coastal, pluvial, and fluvial). We estimated it in the context of the city of Cape Town (South Africa), one of the most exposed cities to pluvial and fluvial flooding in Sub-Saharan Africa. Then, we simulated the adaptation strategies of poor households following an information shock, first at current flood risk conditions, then at revised conditions under climate change. Here is what our results suggest. Information/insurance is effective in helping poor households mitigate the adverse consequences of flood risks, in the face of climate change notably, even if they would further benefit from an improved market access to formal housing. However, their adaptation strategies may aggravate spatial inequalities and reflect an overall deterioration of housing conditions. In the process, we show that distinguishing between flood types is instrumental in understanding households' response in equilibrium.

Considering the production side of the economy, it may therefore be welfare-improving to invest in flood protection. In fact, the type of protection needed differs across flood types. Localized flood risks such as coastal or fluvial risks may be addressed by public investments (e.g., dikes, dams) or urban planning, so as to maintain the attractiveness of certain neighbourhoods. Our model would allow to test the impact and feasibility of such schemes through land value capture.

Figure 13: Absolute change in spatial rent (rands/m²) per housing type under climate change

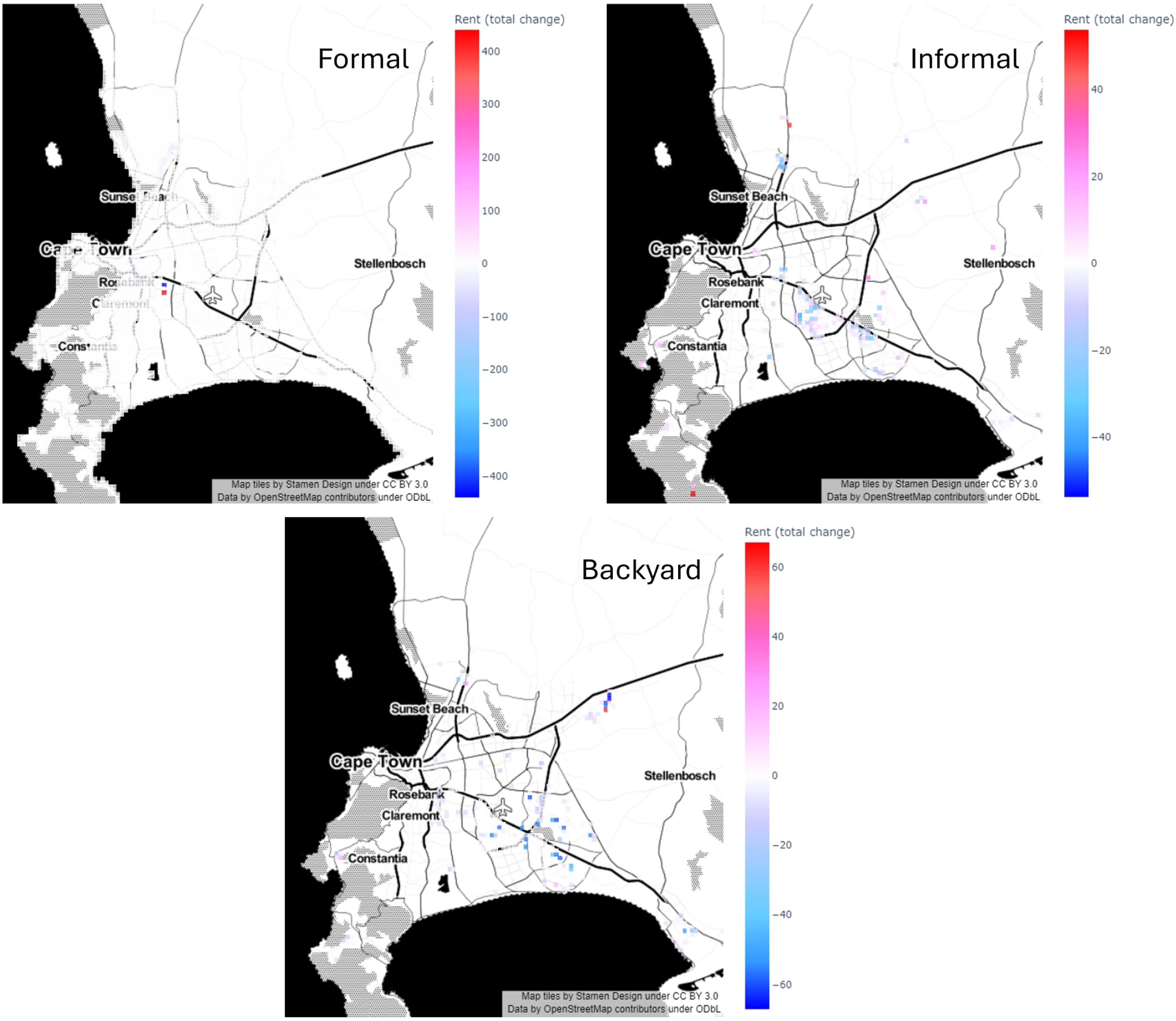

More widespread pluvial flood risks require more global investments in drainage systems and construction technology. In fact, poor households are already responding with private initiatives, especially in informal settlements (e.g., sandbags, barriers, pumps). Local governments could encourage the most effective actions, and our model could help with their identification. These are the main extensions we are considering for future work.

References

Allaire, Maura. 2018. Socio-economic impacts of flooding: A review of the empirical literature. *Water Security*, **3**(5), 18–26.

Avner, Paolo, Mehndiratta, Shomik R., Viguié, Vincent, & Hallegatte, Stéphane. 2017. Buses, houses or cash? Socio-economic, spatial and environmental consequences of reforming public transport subsidies in Buenos Aires. *World Bank Policy Research Working Paper Series*, **8166**.

Avner, Paolo, Hallegatte, Stephane, & Avner, Paolo. 2019. Moral Hazard vs. Land Scarcity: Flood Management Policies for the Real World. *World Bank Policy Research Working Paper*, **9012**(9).

Avner, Paolo, Viguié, Vincent, Arga Jafino, Bramka, Hallegatte, Stephane, & Avner pavner, Paolo. 2022. Flood Protection and Land Value Creation – Not all Resilience Investments Are Created Equal. *Economics of Disasters and Climate Change 2022 6:3*, **6**(3), 417–449.

Bakkensen, Laura A., & Ma, Lala. 2020. Sorting over flood risk and implications for policy reform. *Journal of Environmental Economics and Management*, **104**(11), 102362.

Balboni, Clare. 2025. In Harm's Way? Infrastructure Investments and the Persistence of Coastal Cities. *American Economic Review*, **115**(1), 77–116.

Combes, Pierre Philippe, Duranton, Gilles, & Gobillon, Laurent. 2021. The Production Function for Housing: Evidence from France. *Journal of Political Economy*, **129**(10), 2766–2816.

De Villiers, Gawie, Viljoen, Giel, & Booysen, Herman. 2007. Standard residential flood damage functions for South African conditions. *South African Journal of Science and Technology*, **26**(1), 26–36.

Deltares. 2021. *Planetary computer and Deltares global data: Flood Hazard Maps.*

Ellen, Ingrid Gould, & Meltzer, Rachel. 2024. Heterogeneity in the recovery of local real estate markets after extreme events: The case of Hurricane Sandy. *Real Estate Economics*, **52**(3), 714–752.

Englhardt, Johanna, De Moel, Hans, Huyck, Charles K., De Ruiter, Marleen C., Aerts, Jeroen C.J.H., & Ward, Philip J. 2019. Enhancement of large-scale flood risk assessments using building-material-based vulnerability curves for an object-based approach in urban and rural areas. *Natural Hazards and Earth System Sciences*, **19**(8), 1703–1722.

Epple, Dennis, Gordon, Brett, & Sieg, Holger. 2010. A New Approach to Estimating the Production Function for Housing. *American Economic Review*, **100**(3), 905–24.

Finlay, John, & Williams, Trevor. 2022. Housing Demand, Inequality, and Spatial Sorting. *Imperial College London*, 4.

Fujita, Masahisa. 1989. *Urban Economic Theory: Land Use and City Size*. Cambridge University Press.

Gonzales, Borja, Cian, Fabio, Nyamador, Enock S., Wienhoefer, Kristina, & Carrera, Lorenzo. 2023. *Living on the Water's Edge : Flood Risk and Resilience of Coastal Cities in Sub-Saharan Africa*. World Bank.

Hallegatte, Stephane, Green, Colin, Nicholls, Robert J., & Corfee-Morlot, Jan. 2013. Future flood losses in major coastal cities. *Nature Climate Change*, **3**(9), 802–806.

Hallegatte, Stephane, Rentschler, Jun, & Rozenberg, Julie. 2019. *Lifelines: The Resilient Infrastructure Opportunity*. World Bank.

Hammond, M. J., Chen, A. S., Djordjević, S., Butler, D., & Mark, O. 2015. Urban flood impact assessment: A state-of-the-art review. *Urban Water Journal*, **12**(1), 14–29.

Hino, Miyuki, & Burke, Marshall. 2021. The effect of information about climate risk on property values. *Proceedings of the National Academy of Sciences of the United States of America*, **118**(17).

Huizinga, Jan, De Moel, Hans, & Szewczyk, Wojciech. 2017. Global flood depth-damage functions: Methodology and the database with guidelines. *EU JRC Technical Report*, **105688**.

Kocornik-Mina, Adriana, McDermott, Thomas K.J., Michaels, Guy, & Rauch, Ferdinand. 2020. Flooded Cities. *American Economic Journal: Applied Economics*, **12**(2), 35–66.

Kousky, Carolyn, Kunreuther, Howard, LaCour-Little, Michael, & Wachter, Susan. 2020. Flood Risk and the U.S. Housing Market. *Journal of Housing Research*, **29**(sup1), S3–S24.

Lin, Yatang, McDermott, Thomas K.J., & Michaels, Guy. 2024. Cities and the sea level. *Journal of Urban Economics*, **143**(9), 103685.

Liotta, Charlotte, Viguié, Vincent, & Lepetit, Quentin. 2022. Testing the monocentric standard urban model in a global sample of cities. *Regional Science and Urban Economics*, **97**(11), 103832.

Liotta, Charlotte, Avner, Paolo, & Hallegatte, Stéphane. 2023a. Efficiency and Equity in Urban Flood Management Policies: A Systematic Urban Economics Exploration. *World Bank Policy Research Working Paper*, **10292**(2).

Liotta, Charlotte, Viguié, Vincent, & Creutzig, Felix. 2023b. Environmental and welfare gains via urban transport policy portfolios across 120 cities. *Nature Sustainability*, **6**(9), 1067–1076.

Liotta, Charlotte, Avner, Paolo, Viguié, Vincent, Selod, Harris, & Hallegatte, Stephane. 2024. Climate policy and inequality in urban areas: Beyond incomes. *Urban Climate*, **53**(1), 101722.

Marx, Benjamin, Stoker, Thomas M., & Suri, Tavneet. 2019. There Is No Free House: Ethnic Patronage in a Kenyan Slum. *American Economic Journal: Applied Economics*, **11**(4), 36–70.

Merz, B., Kreibich, H., Schwarze, R., & Thieken, A. 2010. Assessment of economic flood damage. *Natural Hazards and Earth System Sciences*, **10**(8), 1697–1724.

Mosimann, Markus, Frossard, Linda, Keiler, Margreth, Weingartner, Rolf, & Zischg, Andreas Paul. 2018. A Robust and Transferable Model for the Prediction of Flood Losses on Household Contents. *Water*, **10**(11), 1596.

Muller, Nicholas Z., & Hopkins, Caroline A. 2019. Hurricane Katrina Floods New Jersey: The Role of Information in the Market Response to Flood Risk. *NBER Working Paper*, **25984**(6).

Ortega, Francesc, & Taşpınar, Süleyman. 2018. Rising sea levels and sinking property values: Hurricane Sandy and New York's housing market. *Journal of Urban Economics*, **106**(7), 81–100.

Paterson, David L., Wright, Hugh, & Harris, Patrick N.A. 2018. Health Risks of Flood Disasters. *Clinical Infectious Diseases*, **67**(9), 1450–1454.

Pfeiffer, Basile, Viguié, Vincent, Deur, Julien, & Lecocq, Franck. 2019. Could City Population and Containment Favor Gentrification? *CIRED Working Paper*, **72**.

Pfeiffer, Basile, Rabe, Claus, Selod, Harris, Viguie, Vincent, Monnier, Thomas, & Avner, Paolo. 2025. Assessing Urban Policies Using a Simulation Model with Formal and Informal Housing. *Institut Polytechnique de Paris*, 6.

Pharoah, Robyn. 2014. Built-in Risk: Linking Housing Concerns and Flood Risk in Subsidized Housing Settlements in Cape Town, South Africa. *International Journal of Disaster Risk Science*, **5**(4), 313–322.

Picarelli, Nathalie, Jaupart, Pascal, & Chen, Ying. 2017. Cholera in times of floods: Weather shocks and health in Dar es Salaam. *International Growth Centre Working Paper*.

Redding, S., & Rossi-Hansberg, E. 2017. Quantitative Spatial Economics. *Annual Review of Economics*, **9**, 21–58.

Rice, Louis, Scheba, Andreas, & Harris, Adam. 2023. Renting in the informal city: the role of dignity in upgrading backyard dwellings in Cape Town, South Africa. *The Journal of Modern African Studies*, **61**(2), 209–233.

Roux, & Yolandi. 2013. A comparative study of public transport systems in developing countries. *University of Cape Town*.

Sampson, Christopher C., Smith, Andrew M., Bates, Paul B., Neal, Jeffrey C., Alfieri, Lorenzo, & Freer, Jim E. 2015. A high-resolution global flood hazard model. *Water Resources Research*, **51**(9), 7358–7381.

Sturm, Daniel, Takeda, Kohei, & Venables, Anthony. 2023. How Useful are Quantitative Urban Models for Cities in Developing Countries? *London School of Economics*.

Varela, Ana. 2023. Surge of Inequality: How Different Neighborhoods React to Flooding. *London School of Economics & Political Science*, 1.

Viguié, Vincent, & Hallegatte, Stéphane. 2012. Trade-offs and synergies in urban climate policies. *Nature Climate Change*, **2**(5), 334–337.

Viguié, Vincent, Hallegatte, Stéphane, & Rozenberg, Julie. 2014. Downscaling long term socio-economic scenarios at city scale: A case study on Paris. *Technological Forecasting and Social Change*, **87**(9), 305–324.